

CFD Modeling of Gas-Solid Cyclone Separators at Ambient and Elevated Temperatures

Authors:

Mohammadhadi Nakhaei, Bona Lu, Yujie Tian, Wei Wang, Kim Dam-Johansen, Hao Wu

Date Submitted: 2020-04-14

Keywords: elevated temperature process, Computational Fluid Dynamics, cyclone separator, gas-solid

Abstract:

Gas-solid cyclone separators are widely utilized in many industrial applications and usually involve complex multi-physics of gas-solid flow and heat transfer. In recent years, there has been a progressive interest in the application of computational fluid dynamics (CFD) to understand the gas-solid flow behavior of cyclones and predict their performance. In this paper, a review of the existing CFD studies of cyclone separators, operating in a wide range of solids loadings and at ambient and elevated temperatures, is presented. In the first part, a brief background on the important performance parameters of cyclones, namely pressure drop and separation efficiency, as well as how they are affected by the solids loading and operating temperature, is described. This is followed by a summary of the existing CFD simulation studies of cyclones at ambient temperature, with an emphasis on the high mass loading of particles, and at elevated temperatures. The capabilities as well as the challenges and limitations of the existing CFD approaches in predicting the performance of cyclones operating in such conditions are evaluated. Finally, an outlook on the prospects of CFD simulation of cyclone separators is provided.

Record Type: Published Article

Submitted To: LAPSE (Living Archive for Process Systems Engineering)

Citation (overall record, always the latest version):

LAPSE:2020.0373

Citation (this specific file, latest version):

LAPSE:2020.0373-1

Citation (this specific file, this version):



LAPSE:2020.0373-1v1

DOI of Published Version: <https://doi.org/10.3390/pr8020228>

License: Creative Commons Attribution 4.0 International (CC BY 4.0)

Review

CFD Modeling of Gas–Solid Cyclone Separators at Ambient and Elevated Temperatures

Mohammadhadi Nakhaei ^{1,2,*} , Bona Lu ^{3,4}, Yujie Tian ^{3,4}, Wei Wang ^{3,4} , Kim Dam-Johansen ¹ and Hao Wu ¹

¹ Department of Chemical and Biochemical Engineering, Technical University of Denmark, Lyngby Campus, 2800 Kgs. Lyngby, Denmark; KDJ@kt.dtu.dk (K.D.-J.); haw@kt.dtu.dk (H.W.)

² Sino-Danish Center for Education and Research, Beijing 100093, China

³ State Key Laboratory of Multiphase Complex Systems, Institute of Process Engineering, Chinese Academy of Sciences, Beijing 100190, China; bnlu@ipe.ac.cn (B.L.); tianyj@ipe.ac.cn (Y.T.); wangwei@ipe.ac.cn (W.W.)

⁴ Sino-Danish College, University of Chinese Academy of Sciences, Beijing 100049, China

* Correspondence: mnak@kt.dtu.dk

Received: 15 January 2020; Accepted: 7 February 2020; Published: 15 February 2020

Abstract: Gas–solid cyclone separators are widely utilized in many industrial applications and usually involve complex multi-physics of gas–solid flow and heat transfer. In recent years, there has been a progressive interest in the application of computational fluid dynamics (CFD) to understand the gas–solid flow behavior of cyclones and predict their performance. In this paper, a review of the existing CFD studies of cyclone separators, operating in a wide range of solids loadings and at ambient and elevated temperatures, is presented. In the first part, a brief background on the important performance parameters of cyclones, namely pressure drop and separation efficiency, as well as how they are affected by the solids loading and operating temperature, is described. This is followed by a summary of the existing CFD simulation studies of cyclones at ambient temperature, with an emphasis on the high mass loading of particles, and at elevated temperatures. The capabilities as well as the challenges and limitations of the existing CFD approaches in predicting the performance of cyclones operating in such conditions are evaluated. Finally, an outlook on the prospects of CFD simulation of cyclone separators is provided.

Keywords: gas–solid; cyclone separator; computational fluid dynamics; elevated temperature process

1. Introduction

Gas–solid cyclones are frequently used in industrial processes with the primary purpose of two–phase flow separation, i.e., separation of a high-density phase from a lower-density carrier phase, using a turbulent swirling flow. The state-of-the-art industrial cyclone designs are able to operate at elevated temperatures and moderate-to-high loading of solids, while at the same time meeting the required separation efficiency and having low investment and maintenance costs. This has led to the frequent use of cyclones as the only/initial stage of separation and cleaning processes rather than other industrial separators, e.g., bag filters, electrostatic separators, etc. Examples of cyclone separator applications in demanding industrial process conditions are high temperature gas–solid heat exchangers [1], e.g., in the cement industry; gasification and combustion of solid fuels [2–4]; coal pyrolysis [5]; and gas–solid separation in circulating fluidized beds (CFBs) [6].

With the main purpose of gaining improved insight into the flow physics and factors affecting the two important performance parameters of cyclones, i.e., pressure drop and separation efficiency, single–phase and gas–solid flows in pilot-scale cyclones have been extensively studied with the use of experimental methods (for example, see [7–10]). Accordingly, a number of simple semi-empirical/-theoretical models have been proposed to address the flow field and performance

of cyclones (for example see [11–16]), and some of them are still being used in cyclone design and optimization.

In the past two decades, computational fluid dynamics (CFD) has been broadly applied to predict the separation efficiency and pressure drop of cyclone separators and to optimize cyclone designs. Compared to the models based on classical cyclone theory, three-dimensional CFD simulations have the advantage of taking into account the unsteadiness and asymmetry of cyclone flow. On the other hand, the presence of strong swirl and anisotropic turbulent flow as well as adverse pressure gradients in the cyclones has driven the CFD simulation studies to use more advanced turbulence models, e.g., the Reynolds stress transport model (RSTM) and large eddy simulation (LES), as well as higher-order discretization techniques, that are capable of capturing these specific flow physics. These models/techniques, however, are computationally demanding compared to the more commonly used models, e.g., $k-\epsilon$. Furthermore, with the addition of extra physics to the CFD simulation of cyclones, e.g., presence of particles at high loadings and gas–solid heat transfer, additional complications will arise with respect to the solution's accuracy and stability.

In this paper, a brief introduction to the basic operation principles of cyclones at ambient and elevated temperatures is initially presented. Subsequently, the existing CFD simulation studies of cyclones are summarized and discussed based on the operating temperature, i.e., ambient and elevated temperature, and with a special focus on the studies with moderate-to-high loading of particles. The paper highlights specific process parameters that are able to be captured by the CFD simulations at these temperatures. Furthermore, the important sub-models utilized as well as specific challenges that may be encountered in such CFD simulations are addressed.

2. Fundamentals of Gas–Solid Cyclone Separators

The reverse-flow-type gas–solid cyclones are usually equipped with either tangential inlets, which are the main focus in this study, or axial inlets (for example, see [17,18]), usually referred to as swirl tubes [19]. A common configuration of a tangential inlet reverse–flow cyclone is schematically shown in Figure 1a. In this type of cyclone, the swirling gas flow pattern usually consists of a “double vortex”: an outer vortex with a downward axial velocity and an upward-moving inner vortex. The tangential flow pattern, caused by the tangential inlet of the gas to the cyclone system, is referred to as a “Rankine vortex”, comprised of a near-solid-body rotating flow at the core (i.e., tangential velocity is directly proportional to the radius) and a loss-free vortex flow (i.e., tangential velocity is inversely proportional to the radius) at the walls [19] (see Figure 1b). The outer vortex gradually loses its downward momentum in the bottom regions of the cyclone and changes its direction, i.e., “vortex end”, to form the inner vortex. The inner vortex is led to the exit pipe, which is usually extended to the cyclone body to separate the inner vortex from the inlet velocity field. The axial distance from the “vortex end” location to the vortex finder is termed the “natural turning length” [19]. The double vortex structure is inherently unstable due to the presence of a radial pressure gradient imposed by the vortex itself [20]. This phenomenon is referred to as a precessing vortex core (PVC), which causes the location of the vortex axis to oscillate with a specific frequency. In some cyclones, in order to stabilize the vortex end position, a vortex stabilizer is installed either under or above the dust exit location (see Figure 1b), which leads to improved separation efficiency and desirable static pressure below the stabilizer [19].

The static pressure in the cyclone increases monotonically toward the walls to maintain the equilibrium of the rotating flow pattern. This pressure gradient is also present in the boundary layer of the cyclone walls, where the tangential velocity is small [19]. This leads to the presence of a secondary flow, namely inwardly-directed gas flow along the walls, at the cyclone roof, and the conical section, as depicted in Figure 1c.

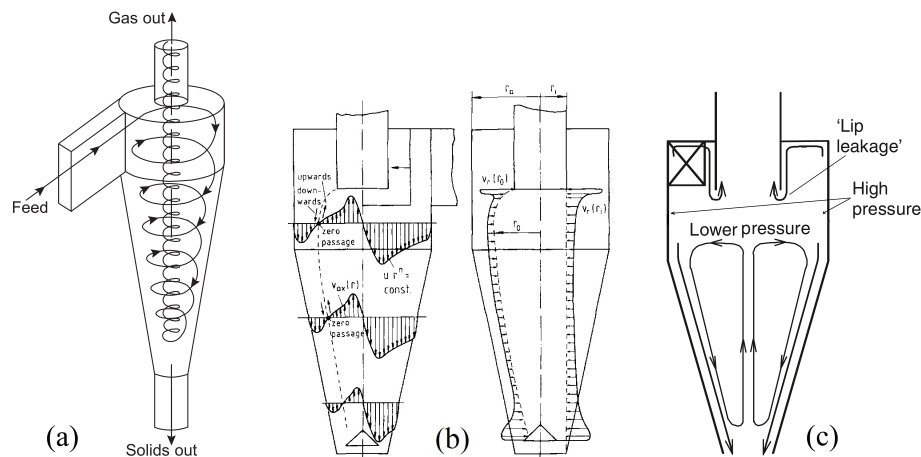


Figure 1. (a) Schematic drawing of a conical reverse-flow cyclone separator illustrating the basic operating principle and the presence of a double vortex inside the cyclone [21], reproduced with permission from G. Towler and R. Sinnott, *Specification and design of solids-handling equipment*, published by Elsevier, 2013. (b) Qualitative patterns of axial, tangential, and radial velocity components of the gas-flow field in cyclones (right) [22], reproduced with permission from M. Trefz and E. Muschelknautz, *Extended cyclone theory for gas flows with high solids concentrations*, published by John Wiley and Sons, 1993. (c) The secondary flow pattern caused by the swirl and pressure gradients in the cyclone [19], reproduced with permission from A. Hoffmann and L. Stein, *Gas Cyclones and Swirl Tubes: Principles, Design and Operation*; published by Springer Nature, 2007.

2.1. Performance Parameters of Cyclones

For the main purpose of gas–solid separation, two important design parameters of reversed-flow conical cyclones are separation efficiency and pressure drop. These parameters are affected by the gas–solid flow field inside the cyclone, which in turn is influenced by the cyclone’s geometrical features as well as the operating conditions. In this section, these performance parameters are discussed and the influences of operating conditions, e.g., solids loading and gas temperature, on cyclone performance are explained.

2.1.1. Separation Efficiency

Cyclone separators are suitable for the separation of solid particles with a size range of 2–2000 microns, which are found in many industries, e.g., heavy industrial smoke, coal dust, cement dust, etc. [19] When solid particles are fed to a cyclone, they are affected by two main forces: the radially outward-directed centrifugal acceleration force, proportional to the cube of particle diameter, and the fluid drag force applied to the particles in the opposite direction; whereas the gravity force is reported to be of minor importance [23]. When the Stokes law applies for the drag force, which is often valid for solid particles in cyclones, the drag force is proportional to the particle diameter. This indicates the dominance of the centrifugal acceleration force for larger particles, leading to their improved separation. The larger particles experience the centrifugal effect as soon as the gas and solids experience the rotational flow at the inlet, and subsequently, they are pushed toward the walls and lose their momentum. Once the particles approach the wall, they start to move downward due to gravity and the drag force applied to them by the downward-directed gas flow. Finally, these particles are separated at the bottom of the cyclone.

Conversely, fine particles, e.g., 1–10 microns, have a greater tendency to follow the gas flow in a cyclone. These particles are poorly separated from the gas phase due to either following the bypass gas to the vortex finder (see Figure 1c) or entrainment to the inner vortex along the inner and outer vortex boundary. The turbulence dispersion of particles intensifies the re-entrainment of fine particles to the inner vortex followed by particle carry over to the vortex finder. On the other hand, the agglomeration of small particles as well as particle attrition can affect the separation efficiency. For example, in the

reported grade efficiencies of a dilutely loaded pilot-scale cyclone, the separation efficiency of particles with a diameter of 0.8–1.0 μm is smaller than the separation efficiency of very fine particles, e.g., 0.3 μm , as well as of large particles [19]. This is known as “fish-hook” behavior [24] and is mainly due to agglomeration of small-sized particles to larger particles, leading to the improved grade efficiency of these particles. The mentioned trend is also observed in other experimental studies [25].

2.1.2. Pressure Loss

One of the main parameters considered in the design of industrial cyclone systems is the energy loss, usually termed the pressure loss. The smaller the pressure loss of the cyclone in a process, the cheaper the process cost. The overall pressure loss in a reversed-flow conical cyclone can be separated into three parts [19,20,26]:

1. Pressure loss at the inlet;
2. Pressure loss in the separation zone;
3. Pressure loss associated with the vortex finder.

The first contributor to the pressure loss is usually of minor importance. The pressure loss in the separation zone is mainly due to the frictional losses at the wall of the cyclone body. The vortex finder pressure loss is due to the dissipation of the swirl dynamic pressure in the vortex finder, which usually takes place without recovering the dynamic pressure into the static pressure. This pressure drop is the main contributor to the overall pressure drop for single-phase flow or dilutely loaded cyclones, and it is proportional to the square of the tangential velocity magnitude. The vortex finder pressure loss is usually affected by the frictional pressure loss, e.g., if the frictional pressure increases due to higher wall roughness or other operating conditions, the vortex will be weakened, leading to the reduction of the vortex finder pressure loss. This indicates that the contribution of different parts of pressure loss changes once the operating conditions of the cyclone change, e.g., an increase in the temperature or the solids loading, which will be further discussed in subsequent sections.

2.2. Effect of Solids Loading on Cyclone Performance

At low solid-to-gas mass loading ratios, e.g., 0.01 kg_s/kg_g , solid particles are clustered as thin strands on the cyclone walls and are transported in the downward direction in a spiral path, while at high mass loadings, e.g., 10 kg_s/kg_g , a major portion of (or the whole) wall surface area is covered with a layer of solid particles (also known as a dense strand in [27]), which is slipped directly into the solids discharge [22]. According to the existing experimental studies of cyclones, both overall and grade separation efficiencies are improved by increasing the inlet solids mass loading ratio [7,8,19]. Hoffmann and Stein [19] reported an overall improvement of the grade efficiency of almost all particle sizes for an increase in the inlet particle mass loading from 3.7×10^{-3} to 2.6×10^{-2} kg_s/kg_g . However, they have stated that the separation efficiency at high mass loading of particles is somewhat dependent on the inlet gas velocity of the cyclone, i.e., the swirl strength [28]. The overall separation efficiency versus inlet solids loading of selected experimental studies is presented in Figure 2. In this figure, the improvement of separation efficiency with the cyclone Reynolds number can be observed from the experimental data of [19] for a fixed value of kinematic response time of particles of $\tau_p = \frac{\rho_p d_p^2}{18 \mu_g} = 0.1$ milliseconds. The improvement is more noticeable for lower mass loadings, i.e., below 0.01 kg_s/kg_g . The kinematic response time of particles used in the study of Fassani and Goldstein [29] is somewhat higher compared to the particles of other studies presented in Figure 2, leading to a very high efficiency of separation. For the rest of the studies, no conclusive argument can be stated regarding the effect of this parameter.

Despite available experimental studies on the effect of solids loading on the separation efficiency, there is no consensus regarding the exact mechanism of this improvement [19]. According to the concept of the critical mass loading ratio, ϕ_G , initially introduced by Muschelknautz and Brunner [8,13],

when the inlet particle mass loading is higher than the critical mass loading, the share of particles corresponding to the extra amount of mass loading is ideally separated at the cyclone inlet, while the rest of the particles are separated based on a balance between the centrifugal forces and the turbulent dispersion, commonly referred to as “inner separation” [22]. The concept of Muschelknautz, however, suggests that the separation efficiency is independent of the mass loading for loadings smaller than ϕ_G , which is not consistent with the experimental data in the literature [28]. On the other hand, based on another concept introduced by Mothes and Löffler [30], the improvement in the separation efficiency at high solid mass loadings is attributed to the agglomeration of smaller particles, i.e., 2 μm diameter and smaller, to larger particles, i.e., 15 μm diameter. Hoffmann and Stein [19] interpreted the separation efficiency of cyclones at high mass loadings to be a combined effect of different contributions. For very fine particles, the agglomeration effect is more dominant, leading to a high efficiency of these particles, especially for a humid carrier gas [19]. Furthermore, they argued that the increased concentration of particles at the inlet can lead to reduced drag force, which improves the separation process.

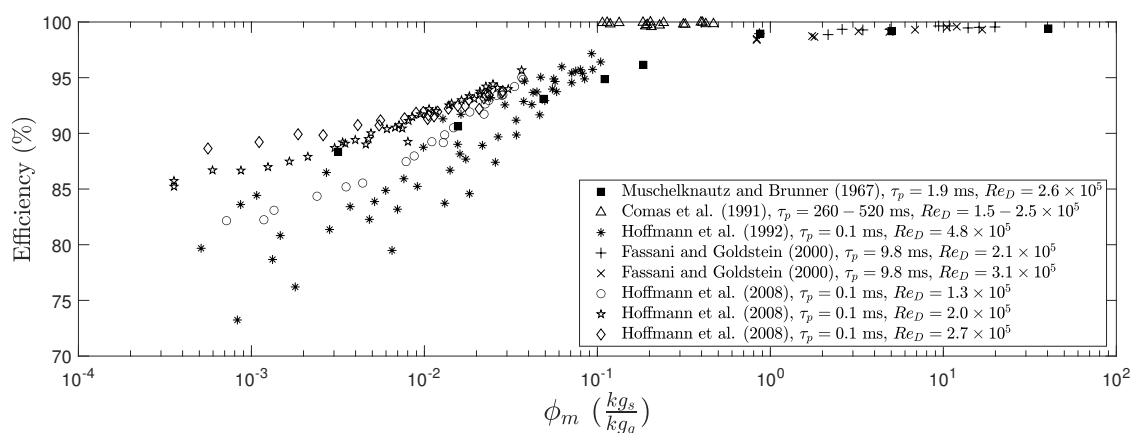


Figure 2. Overall cyclone separation efficiency versus mass loading ratio at the cyclone inlet for selected experimental data in the literature [7,8,19,29,31]. The Reynolds number is calculated based on the inlet velocity and the cyclone body diameter.

Baskakov et al. [32] and Muschelknautz and Brunner [8] have reported a decrease in the pressure drop up to a specific amount of solids loading, followed by an increase. A similar trend is also observed in other experimental [33] and CFD simulation studies [34,35]. This behavior is attributed to the increase of the frictional pressure loss due to the presence of particles near the walls. Although, at the same time as the friction velocity at the cyclone walls increases, the swirl intensity is weakened; consequently, the pressure loss associated with the vortex finder is decreased. Muschelknautz and Brunner [8] reported an 85% reduction in the tangential velocity peak by increasing the solids loading from 0 to around 20 kg_s/kg_g . At low mass loadings, the decrease in the vortex finder pressure loss is more pronounced, leading to the reduction of the overall pressure loss, whereas when the particle mass loading is sufficiently high, the vortex finder pressure loss becomes negligible due to a very weak tangential swirl and the frictional pressure drop still increases with the loading of particles [35]. As a consequence, the overall pressure drop starts to increase with the solids loading after reaching a minimum value.

A summary of selected experimental data on pressure drop versus solids loading in pilot-scale cyclones from the literature is presented in Figure 3. Despite the mentioned explanation, there are other studies in the literature that dispute the presence of a minimum pressure drop when the loading of particles changes. For example, in some studies [7,9,10,31], it is reported that by increasing the mass loading of particles in the cyclone, the pressure drop is reduced, although these studies are limited to small mass loadings, e.g., up to 0.5 kg_s/kg_g in [31], 0.1 kg_s/kg_g in [7], and 0.2 kg_s/kg_g in [9]. The mass loading ratio at which the minimum pressure drop occurs is reported to be around 0.25 (at an operating gas temperature of 250 $^{\circ}\text{C}$) and 2.0 (at ambient temperature) in the studies of Baskakov et al. [32] and

Muschelknautz and Brunner [8], respectively. Furthermore, in some of the studies, it is reported that by increasing the inlet solids loading, the pressure drop increases [36] or remains at a nearly constant value lower than the pressure drop of the single-phase flow cyclone [29].

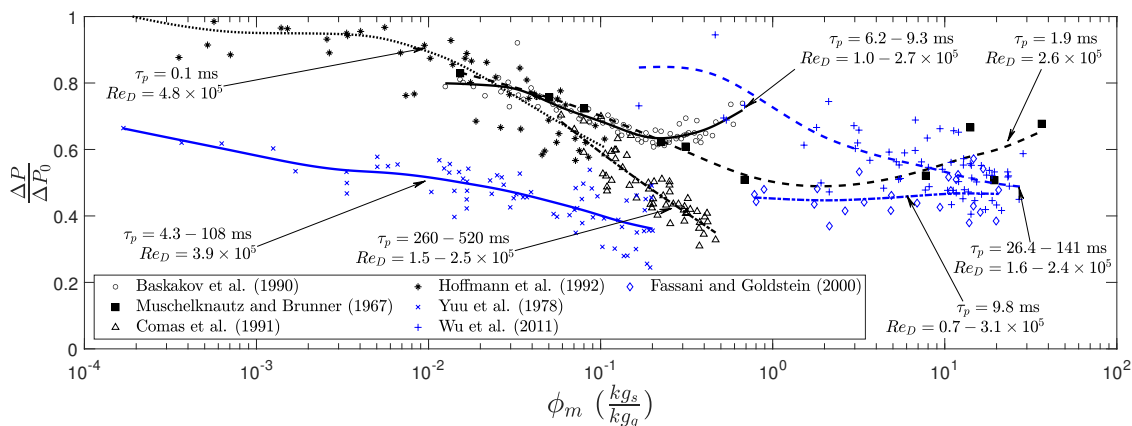


Figure 3. Experimental data of pressure drop (normalized with the pressure drop of a particle-free cyclone, ΔP_0) versus mass loading of pilot-scale cyclones from selected studies [7–9,29,31,32,37]. The lines are numerical fits to each set of experimental data. The Reynolds number is calculated based on the inlet velocity and the cyclone body diameter.

2.3. Effect of Operating Temperature on Cyclone Performance

The use of gas–solid cyclones is popular in high-temperature industrial processes, e.g., for drying, solidification, heating, flue gas cleaning purposes, etc. The high-temperature cyclone separators can be loaded with large amounts of particles, e.g., in gas–solid CFB cyclones, the solids loading can be on the order of 10–100 kg_s/kg_g [38]. As briefly mentioned earlier, the cyclone’s performance is affected by its operating temperature. In this section, a brief introduction to the effect of cyclone gas temperature on separation efficiency, pressure drop, and gas–solid heat transfer is provided.

In general, as gas temperature rises, gas density and viscosity are, respectively, decreased and increased. At a fixed volumetric gas-flow rate to the cyclone, a direct consequence of this change in the fluid properties is the reduction of the cyclone’s Reynolds number and the swirl intensity in the cyclone at elevated operating temperatures. As a result, the cyclone’s pressure drop is reduced. This trend is reported in many experimental [39,40] and CFD studies (for example, see [41]) of cyclones operating at elevated temperatures.

For a fixed inlet gas velocity to the cyclone, as the temperature increases, the particle cut-size, i.e., the diameter at which the cyclone separation efficiency is equivalent to 50%, increases, indicating a negative influence of the operating temperature on the separation efficiency [39,40]. This behavior can be partly attributed to an intensified drag force applied to the particles by the carrier fluid as a consequence of increased gas viscosity at elevated temperatures. Furthermore, as stated before, the reduction in the swirl intensity leads to a weaker centrifugal effect on the particles compared to the intensified drag force, and as a result, the separation efficiency is reduced [40]. On the other hand, the gas density is inversely proportional to the temperature; but its effect on particle separation is less significant as only the difference between the gas and particle densities is the determining factor on the buoyancy force applied to the particles.

In the existing experimental studies in the literature, the heat transfer rate to the particles in gas–solid cyclone heat exchangers is positively affected by the loading of particles and the inlet gas velocity, while being inversely influenced by the particle size [1]. Improvement in the heat-transfer rate with solids loading is attributed to the reduced radial gas velocity in the cyclone as a result of stronger gas–solid momentum coupling. Consequently, the amount of gas bypassed to the vortex finder at the entrance of the cyclone is reduced, leading to the presence of a higher-temperature gas at the bottom regions of the cyclone and further improvement in the heat-transfer rate to the solids [1]. As the

particle loading further increases, the rate of increase in the gas–solid heat transfer rate reduces [1,42] and approaches a certain value. Increased gas–solid heat transfer as a result of higher inlet gas velocity as well as the reduction of particle size can be simply explained by an improved driving factor for gas–solid heat transfer, i.e., more availability of the high temperature gas to transfer heat to the solids and improved gas–solid surface area for heat transfer, respectively.

One of the challenges that may exist at the cyclone’s internal walls, especially for cyclones operating at elevated temperatures, is erosion due to wall–particle collision and/or corrosion due to the presence of aggressive species and agents in the gas, even in the presence of a strong refractory lining. It is more likely to have erosion on the cyclone wall in front of the gas inlet, caused by the very first impact that solids have with the cyclone wall, followed by a change in the direction of particle movement [43]. An immediate outcome of cyclone wall erosion is more rough surfaces on a cyclone’s internal walls, affecting the pressure drop and separation efficiency of particles. A common solution for this challenge is “hardware” changes in the cyclone system during the maintenance period, e.g., installation of wear plates and replacement of eroded materials [19]. Furthermore, cyclone design modification is an option to improve the erosion behavior, e.g., adding a flat-disk vortex stabilizer close to the particle outlet reduces erosion [44]. Apart from erosion and corrosion, the deposition of particles on the cyclone walls can induce operational challenges in the long term. Deposit formation can take place on the outer surface of a vortex finder [45], dipleg [46], or on the internal walls of the cyclone body [47].

3. Approaches for the Numerical Modeling of Gas–Solid Systems

The use of numerical simulations is undoubtedly a valuable tool for understanding and improving industrial gas–solid systems. However, the presence of a very large span for length and time scales of both phases, which are influenced by each another, makes resolving all of the details of a gas–solid system through computational simulation a challenging task [48]. In the existing numerical methods, the gas–solid flow is resolved at different but limited ranges of length and time scales, and the smaller-scale details, if any, are modeled. A summary of the available approaches for a four-way coupled (to be explained later) gas–solid system is provided in Table 1. In the most fundamental approach, usually referred to as direct numerical simulation (DNS), the boundary layer over the particles surface is resolved. DNS can itself be categorized into two approaches: the resolved Eulerian–Lagrangian model, e.g., immersed boundary model, and the Lagrangian–Lagrangian approach using molecular dynamics, e.g., Lattice Boltzmann, applicable for simulations of gas–solid flows at extremely small scales of 0.01 and 0.001 m, respectively [48]. DNS is usually utilized for fundamental studies of gas–solid flows at small scales in order to develop sub-models, e.g., drag and Brownian motion models, for more simplified approaches.

In the Eulerian–Eulerian (E–E) approach, both phases are described as a continuum medium and solved in an Eulerian domain [49], while the gas–solid interactions are incorporated through a drag model and the particle–particle interactions through models for solid pressure and viscosity, e.g., the kinetic theory of granular flows (KTGF) [50]. A challenge in using the basic formulation of the E–E approach is the difficulty in taking into account poly-disperse particles in the model. However, there are several sub-models, such as the population balance model (PBM), that can be added to the basic E–E equations to account for different particle sizes, with the cost of higher computational overhead since separate momentum and continuity equations should be solved for each size bin [51–53]. In addition, some complex physical phenomena such as particle agglomeration and break-up can be modeled in combination with the PBM [54]. A limitation of the E–E approach is the validity of the continuum hypothesis for both phases, i.e., both phases are adequately present over the whole computational domain. This makes the model more appropriate for gas–solid systems with more homogeneous distributions of particles, mainly dense gas–solid systems such as fluidized beds.

In the (unresolved) Eulerian–Lagrangian (E–L) approach, also referred to as the discrete particle model (DPM), the carrier gas flow field is considered as a continuum medium and solved using

an Eulerian formulation, while solid particles are tracked in a Lagrangian platform using Newton’s second law. Compared to the resolved E–L model, categorized as DNS in this study, the boundary layer over the particle surface is not resolved in the unresolved E–L and the size of the computational grid is significantly larger than the particle size. One distinct advantage of this model compared to the E–E approach is the direct resolving of particle movement, i.e., fewer closure models are employed for the particle phase, which makes the model more accurate. Furthermore, poly-disperse systems can be readily modeled using the E–L method. The particle–particle interactions in the E–L model are usually incorporated as either hard-sphere or soft-sphere collision models. In the hard-sphere model, the collisions take place instantly and can be employed in both stochastic and deterministic collision approaches; thus it is suitable for dilute flows where binary collisions happen. Conversely, this model is not suitable for cases where particles go through multiple collisions with other particles simultaneously. The soft-sphere model, also referred to as the discrete element model (DEM), is a deterministic particle collision approach that takes into account overlapping particles during the collision and is able to incorporate multiple simultaneous collisions for a particle [55]. As the loading of particles in a gas–solid system increases, the E–L approach becomes computationally expensive, especially if the DEM model is utilized [55].

As an alternative, the particle–particle interactions can be modeled by using hybrid E–E and E–L approaches, such as the multi-phase particle in-cell (MP-PIC) method [56–58] and the dense discrete phase model (DDPM) [59]. The basic idea in the hybrid approach is to solve the carrier phase in an Eulerian frame with the inclusion of the particle phase volume fraction, taken from the Lagrangian tracking, in the conservation equations. Similar to the E–L method, the particles are tracked in a Lagrangian frame, while the particle–particle interactions are modeled using solid stress calculated from the Eulerian grid [58,59]. Since the interparticle interactions are modeled instead of being directly resolved, the computational overhead of the solution is reduced compared to the unresolved E–L approach, while the model is superior over the E–E model (e.g., straightforward handling of poly-dispersed particles).

Table 1. Summary of the available approaches for computational fluid dynamics (CFD) simulation of gas–solid flows with the inclusion of closure models to be considered in each approach. The table is inspired from [60].

	Gas-Solid CFD approaches	Closure models	Comments
	<div style="border: 1px solid black; border-radius: 10px; padding: 5px; width: fit-content; margin-bottom: 10px;"> Quasi single-phase model (mixture model) </div>	<ul style="list-style-type: none"> - Mixture properties model - Slip velocity - Drag model 	<ul style="list-style-type: none"> - Only applicable for very dilute systems - Usually inaccurate results
	<div style="border: 1px solid black; border-radius: 10px; padding: 5px; width: fit-content; margin-bottom: 10px;"> Eulerian-Eulerian model (two-fluid model) </div>	<ul style="list-style-type: none"> - Drag model - Pressure viscosity closure (e.g., kinetic theory model) 	<ul style="list-style-type: none"> - Continuum hypothesis should be valid, i.e., the gas and solid phases should be sufficiently present in each control volume - Usually carried out for mono-dispersed particles as employing a poly-dispersed particle size is limited by the computational overhead
	<div style="border: 1px solid black; border-radius: 10px; padding: 5px; width: fit-content; margin-bottom: 10px;"> Unresolved Eulerian-Lagrangian model (DPM) </div>	<ul style="list-style-type: none"> - Drag model - Stochastic or deterministic collision model 	<ul style="list-style-type: none"> - Reduced computational overhead compared to E-L models with resolved particle-particle collisions - Computationally expensive for large systems especially with deterministic collision models
	<div style="border: 1px solid black; border-radius: 10px; padding: 5px; width: fit-content;"> Direct numerical simulation: • Resolved Eulerian-Lagrangian model (e.g., immersed boundary models) • Lagrangian-Lagrangian model (e.g., Lattice Boltzmann) </div>	<ul style="list-style-type: none"> - No closure 	<ul style="list-style-type: none"> - Extremely expensive - Can be used for development of closure models, e.g., drag

4. CFD Simulation Studies of Gas–Solid Cyclones at Ambient Temperature

When solid particles are added to the gas flow in a cyclone separator, the mean and turbulent properties of the flow field may change. According to the classification of gas–solid interactions made by Elghobashi [61] (see Figure 4), for particle volume fractions lower than 10^{-6} (equivalent to the interparticle spacing of around $80d_p$ [20]), particles have a negligible influence on the turbulent flow field, and the gas–solid coupling is termed as one-way coupling. When the particle volume fraction reaches values higher than 10^{-6} but below 10^{-3} (equivalent to the interparticle spacing of around $8d_p$ [20]), the particles either attenuate or intensify the turbulence in the gas–solid flow, i.e., two-way coupled flow field, depending on the relative kinetic response time of particles to the characteristic flow time-scale [61]. In the context of gas–solid cyclone flows, attenuation is usually the case [20]. If the solids volume fraction is increased further, namely to the four-way coupling region, the interaction between particles becomes important too.

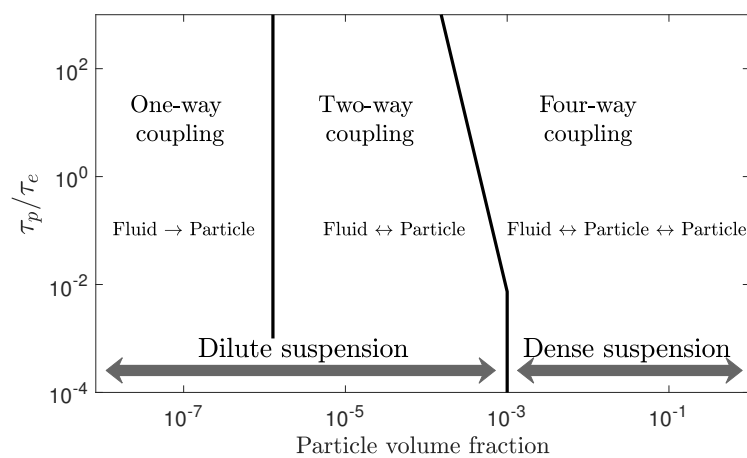


Figure 4. Map of gas–solid interaction regimes of particle-laden turbulent flows. τ_p and τ_e are the particle kinetic response time and time-scale of large eddies in a turbulent flow, respectively. Reproduced with permission from S. Elghobashi, On predicting particle-laden turbulent flows; published by Springer Nature, 1994 [61].

There are a vast number of CFD simulation studies of cyclone separators at ambient temperature, which are usually carried out for pilot-scale cyclone designs. In the current study and according to the above classification, these studies are separated into three groups of (I) single-phase gas flow; (II) one-way coupled gas–solid flow; and (III) two- and four-way coupled gas–solid flow in cyclones.

4.1. Group I: Single-Phase Flow CFD Simulations

As briefly mentioned earlier, the turbulent flow inside a particle-free conical cyclone is anisotropic and inherently unsteady due to the significant swirl and radial shear intensity as well as the adverse pressure gradient, which may induce recirculation regions. Accordingly, the turbulence model utilized in the CFD simulation of cyclones should be capable of correctly resolving or modeling the high curvature and intensive swirl flow and, at the same time, would be appropriate for modeling the adverse pressure gradient and recirculating flows [20].

As a result of being based on an isotropic turbulent flow assumption, the commonly used classical first-order turbulence models of the steady-state and unsteady Reynolds-averaged Navier–Stokes equations (URANS), i.e., zero-, one-, and two-equation models such as the k - ϵ model, are usually unable to accurately reproduce the flow field inside cyclones [62–65]. However, there are some attempts that have been carried out to improve the accuracy of the first-order turbulence models with the inclusion of anisotropy effects in their modified versions, e.g., the k - ϵ model based on renormalization group (RNG) theory [63,65], the k - ϵ curvature correction (cc) model [66], and the model proposed by Meier and

Mori [67]. These models provide improved accuracy in the prediction of single-phase flow in cyclones compared to the standard two-equation models. Alternatively, the second-order URANS closure models, e.g., the Reynolds stress transport model (RSTM) [66,68–70] and scale-resolving turbulence models, e.g., large eddy simulation (LES) [71,72], are able to capture the anisotropy effects in highly swirling flows and have been proven to be accurate in predicting the cyclone gas flow field. Among the two widely used variations of the differential RSTM in modeling the pressure-strain term, i.e., the Launder, Reece, and Rodi (LRR) model [73] and the Speziale, Sarkar, and Gatski (SSG) model [74], the latter provides superior accuracy [66]. With the recent advancements in computer capabilities, the use of LES for the prediction of the flow inside cyclones has become possible, but with a higher computational overhead cost. Using LES, it is possible to study cyclone flow physics in extensive detail and the accuracy of results is superior compared to the RSTM [75–77]. Nonetheless, the RSTM can provide reasonable predictions of the gas flow in cyclones using a relatively coarser computational grid compared to the ones used in LES studies, and at a much lower computational overhead than LES [76].

Apart from the turbulence model, there are important considerations related to the numerical aspects of CFD simulations of gas flow in cyclones. Due to the presence of strong velocity and pressure gradients, the use of high-order (i.e., second order and above) methods in the discretization of advection terms as well as the alignment of the computational cells with the flow direction (i.e., structured grids) are recommended in order to avoid unwanted numerical diffusion (for example, see [78]).

There are a large number of existing CFD studies focusing on single-phase flow characteristics in cyclones that are not fully listed here as it is not the main subject of this review. A summary of some of the previous single-phase flow studies, up to 2007, can be found in [20].

4.2. Group II: One-Way Coupled Gas–Solid Flow Simulations

In the second category of existing CFD studies of cyclones operating at ambient temperature, category (II), the one-way coupling method is employed for very dilute loading of particles (see Figure 4), and the E–L approach is commonly utilized. The particles are tracked either after the simulation has reached a steady-state solution, as a post-processing step [69,79–87], or in a transient way along the unsteady simulation [75,79,88–93]. After the completion of the particle-tracking procedure, the particle separation efficiencies are predicted and usually compared with the available experimental data. In general, it can be stated that there is a tendency for the particle cut-size diameter to be underpredicted in LES calculations [88,89,93] and overpredicted in RSTM calculations [20,93]. Furthermore, the separation efficiency is predicted more accurately when LES is used [93], due to a better prediction of the mean and fluctuating velocity fields. One must keep in mind that the accuracy of the predicted separation efficiency, however, depends on the validity of the basic assumptions for the simulations, e.g., the accumulation of particles near the cyclone walls may cast doubt on the validity of the one-way coupling assumption.

An important consideration in one-way coupled E–L simulations is the influence of turbulent dispersion, i.e., the movement of particles due to the presence of velocity fluctuations, especially for smaller-sized particles. If the resolved scales have comparable time-scale as compared to the kinematic response time of particles, e.g., LES and DNS, the turbulent dispersion is resolved directly and no additional turbulent dispersion model is required [79,94], while the effect of sub-grid scale (SGS) structures in LES on particle movement can usually be neglected. For URANS simulations, however, it is common to apply a stochastic turbulent dispersion model [95]. Accurate prediction of the gas velocity fluctuations, i.e., rms velocities, is important for properly resolving particle dispersion due to turbulence. In some of the existing studies, it is reported that even though the mean velocities are properly captured by the RSTM, the rms fluctuations of the velocity field are underpredicted compared to the measurements [76,96], due to a failure in accurately predicting PVC behavior that gives rise to the rms velocities, especially in central regions of a cyclone [76]. Shukla et al. [96] reported

an overprediction of separation efficiency for smaller-sized particles due to an underprediction of velocity fluctuations, as shown in Figure 5. On the other hand, LES is able to capture both mean and rms velocities properly, leading to accurate predictions of grade efficiency compared to the measurements [96].

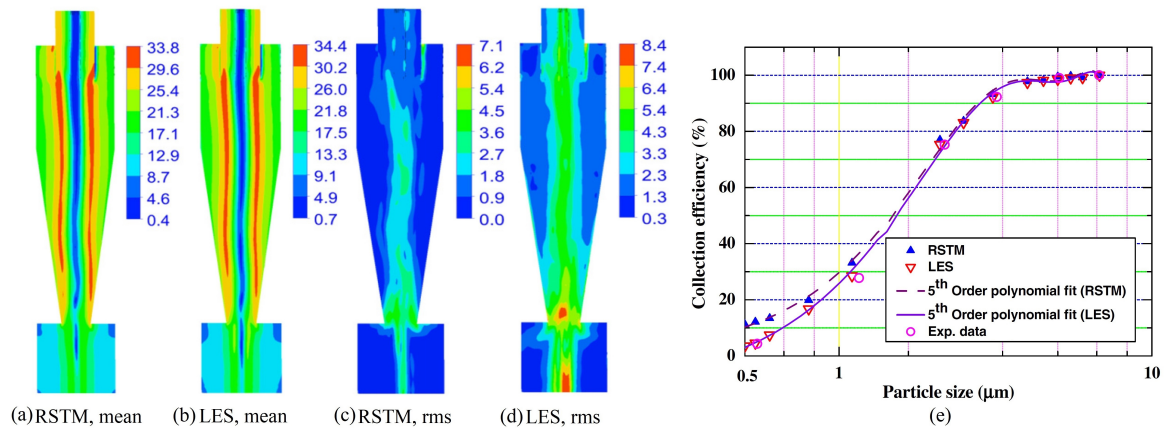


Figure 5. Comparison of predicted mean velocity profiles (a,b), rms velocities (c,d), and grade efficiencies (e) using the Reynolds stress transport model (RSTM) and large eddy simulation (LES) for a cyclone with a body diameter of 0.29 m and operating at ambient temperature and pressure [96]. The experimental data on separation efficiency are from [97]. Reproduced with permission from S. Shukla et al., The effect of modeling of velocity fluctuations on prediction of collection efficiency of cyclone separators; published by Elsevier, 2013.

4.3. Group III: Two- and Four-Way Coupled Gas–Solid Flow Simulations

Both the E–E and the E–L methods are employed for CFD simulation of two- and four-way coupled gas–solid flows. Generally speaking, and as discussed earlier, the volume fraction of particles in a cyclone separator is locally inhomogeneous, as the design of such equipment demands. Consequently, in the existing studies of cyclone separators, the E–L approach is preferred over the E–E approach.

4.3.1. E–L and Hybrid Model Simulations

As for the third category of CFD studies, category (III), compared to the previous categories, there are fewer E–L studies with two-way coupling [34,77,98–105] and only a limited number of studies with four-way coupling [35,106–109]. In almost all of the studies (except [99]), due to the lack of available experimental data for the cyclone flow loaded with particles, no comparison of the predicted modification of velocity profiles (compared to the single-phase flow) with the measurements is provided. Instead, the predicted overall/grade efficiencies [34,77,101,102] and/or pressure drops [34,35,98,101,102,106,107,109] are compared with the measurements for certain ranges of particle mass loading. A summary of the existing four-way coupled CFD studies of gas–solid cyclones operating at ambient temperature and with inlet mass loading ratios higher than 0.1 kg_s/kg_g is presented in Table 2.

Table 2. Details of the selected CFD studies of gas–solid flow in cyclones operating at ambient temperature with the four-way coupling method, in chronological order.

Author(s)	Cyclone Dimensions, D × H (m ²)	Cyclone Re Number ^(a)	Particle Diameter (μm)	Inlet Mass Loading (kg _s /kg _g)	CFD Solver	Turbulence Model/Turbulent Dispersion	Drag Model	Validation/Comments
Chu et al. [109]	0.2×0.8	272,000	2000 (mono-sized)	up to 2.5	ANSYS FLUENT (computational fluid dynamics–discrete element model, CFD–DEM, + user–defined functions, UDF)	Reynolds stress turbulent model, RSTM/not mentioned	friction and pressure gradient drags + particle rotation	Pressure drop is compared with the experiments for particle-free and particle-laden flows with solids loadings in the range of 0–2.5 kg _s /kg _g
Schneiderbauer et al. [110]	2.5×6.0	817,000	0.6–400 (size range)	0.22	ANSYS FLUENT 16 (hybrid Eulerian–Eulerian, E–E, and Eulerian–Lagrangian, E–L)	RSTM/not mentioned	heterogeneous model of [111]	Predicted grade and overall efficiencies are compared with the measurements. The implemented agglomeration model is reported to be crucial for proper prediction of grade efficiency, while the predicted overall efficiency is not influenced by presence of the agglomeration model.
Wei et al. [112]	0.3×1.1	113,000–263,000	2000 (mono-sized)	0.72–8.64	ANSYS FLUENT 15.0 coupled with EDEM 2.7 (CFD–DEM)	RSTM/not mentioned	Gidaspow [50]	Predicted pressure drops are compared with the experimental data for solids loadings of 0.72–8.64 kg _s /kg _g . Presence of solid strands and an ash top ring are reported.
Kozolub et al. [106]	0.2×0.78	75,300–130,000	2000 (size range)	0.61–2.9	ANSYS FLUENT 13.0 (dense discrete phase model, DDPM, based on kinetic theory of granular flow, KTGF)	RSTM/not mentioned	Wen–Yu [113]	Pressure drop is compared with the experimental data for particle-free and particle-laden flows with solids loadings in the range of 0–2.9 kg _s /kg _g . For the particle-laden flow, the trend of pressure drop change is well predicted while the values are somewhat overpredicted.
Sgrott and Sommerfeld [108]	0.29×1.16	280,000	0.5–60 (size range)	0.1	OpenFOAM 2.3.1 (CFD–DEM + agglomeration)	Large eddy simulation, LES/isotropic Langevin model	not mentioned particle rotation	For a particle-free flow, the predicted velocity profiles are compared with the experimental data of [114]. No validation is given for the particle-laden simulation case.
Zhou et al. [107]	0.29×1.16	30,000–188,000	2000–2800 (size range)	0.07–0.46	ANSYS FLUENT 6.3 (CFD–DEM)	RSTM/not mentioned	Gidaspow [50] particle rotation lift force	The predicted velocity profiles of a particle-free flow are compared with the experimental data of [114]. The pressure drop of the particle-free and particle-laden cases is compared with the measurements, while the difference between the particle-free and particle-laden pressure drops is not significant.
Hwang et al. [35]	0.2×0.8	272,000	2000 (mono-sized)	up to 20	ANSYS FLUENT 16.2 (DDPM–KTGF)	RSTM/discrete random walk, DRW	Wen–Yu [113]	The predicted pressure loss is compared with the experimental and numerical data of [109] for solid mass loadings up to 2.5.

^(a) The Reynolds number is calculated based on the inlet velocity and the cyclone body diameter.

Effect of Solids Loading

As the solids loading ratio increases, the particle–particle interactions become important and neglecting these interactions in the cyclone CFD simulation may lead to poor predictions of cyclone performance. For example, Wasilewski and Duda [115] have reported an underprediction of both pressure drop and separation efficiency for two different pilot-scale cyclone geometries, though the overall trend of changes was well-predicted. The authors have claimed that this discrepancy is due to the simplification of the CFD model, neglecting particle–particle collisions and agglomeration. Both CFD–DEM [107–109] and hybrid E–E and E–L approaches [35,106] have been used to consider the effect of particle–particle interactions in existing cyclone separator simulation studies. In the CFD–DEM study of Zhou et al. [107], the effect of large (2000–2800 μm) and “ultra light” particles with a solid to gas density ratio of 33 is investigated for different loadings of particles up to 0.46 kg_s/kg_g . They have analyzed the significance of gas–solid and solid–solid forces in different regions of cyclones and concluded that the modification of the velocity field due to the presence of particles is hardly noticeable. On the other hand, based on CFD–DEM calculations, Chu et al. [109] reported a significant modification of the velocity field due to the presence of particles of nearly the same size but much heavier compared to the ones studied in [107]. According to this study, the particle–particle forces, which are much more dominant than the particle–gas forces, increase in magnitude with the loading of particles, with the most active region being inside the particle strands along the cyclone wall.

In most of the existing four-way coupled CFD simulations of cyclones using the hybrid methods [35,106], the focus is on the effect of solids loading on the performance of cyclones. Hwang et al. [35] carried out DDPM–KTGF simulations of a pilot-scale cyclone laden with 2000 μm diameter particles and reported a minimum in the predicted pressure drop versus solids loading. The comparison with available measurements, though, is carried out only for smaller solids loadings, i.e., loadings smaller than 2.5 kg_s/kg_g , while the minimum pressure drop takes place at solids loadings of around 6 kg_s/kg_g . Conversely, in the hybrid E–E and E–L study of Kozolub et al. [106], an increasing trend in the predicted pressure drop of a cyclone laden with 40–80 μm diameter particles is observed for all of the studied mass loadings up to 2.6 kg_s/kg_g . This trend is in line with the available measurements, but the values are somewhat underpredicted.

One of the important features that is captured by two- and four-way coupled CFD simulations of cyclones is the modulation of velocity field and turbulence statistics as compared to the particle-free flow. The swirl velocity is predicted to reduce substantially with the addition of particles to the flow and decrease further as the loading of particles increases [35,102,106,109,116]. The predicted reduction of tangential velocity magnitude as well as turbulent fluctuations by the addition of 0.05 and 0.1 kg_s/kg_g of particles to a pilot-scale cyclone is shown in Figure 6 based on the LES study of Derksen et al. [116]. The reduction of swirl is reported to be stronger in the loss-free vortex part of the swirl due to the higher concentration of particles in this region. On the other hand, the tangential velocity at regions close to the walls is still high (see Figure 6) due to the presence of particles and partial transfer of tangential momentum to the gas phase. The reduction of swirl can, in turn, reduce the effectiveness of centrifugal force on particle separation in the cyclone, making the particles be less concentrated near the walls. However, at the same time, the turbulence is attenuated by the presence of particles all over the cyclone body [116], leading to the reduction of turbulent dispersion; also, the amount of gas bypassed to the vortex finder at the entrance of the cyclone is reduced. The overall separation efficiency with respect to the solids loading is a balance between the significance of the above-mentioned effects.

The modification of cyclone efficiency with particle mass loading is not reported in the existing four-way coupled CFD studies as in most of the studies [35,107,109], the addition of large particles to the cyclone, e.g., 2000 μm in diameter, is investigated, leading to an ideal separation efficiency.

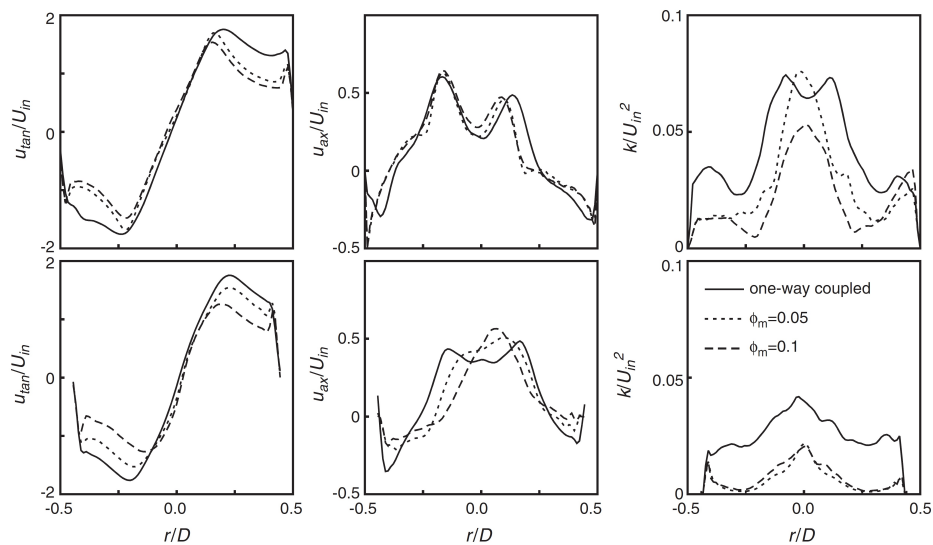


Figure 6. The predicted time-averaged values of axial and tangential velocities as well as the resolved turbulent kinetic energy of the gas for a pilot-scale cyclone with a body diameter of 0.29 m and operating with different mass loadings of particles using two-way coupled LES at 0.75D (top) and 2D (bottom) below the cyclone roof [116]. Reproduced with permission from J.J. Derksen, Simulation of mass-loading effects in gas-solid cyclone separators; published by Elsevier, 2006.

Agglomeration of Particles

As mentioned earlier, an important mechanism in solids separation in cyclones is particle agglomeration [19,30]. To model the particle agglomeration in a Lagrangian frame, it is common to assume either volume-equivalent (i.e., the new diameter has the same volume as the agglomerated particles) [117,118] or inertia-equivalent (i.e., the new diameter is calculated to maintain the inertia) [108,119,120] agglomeration. The agglomeration of particles in cyclones is studied in the CFD–DEM simulations of Sgrott and Sommerfeld [108] with a stochastic approach [121] to describe the particle–particle collisions. It is assumed that the only driving factor in interparticle adhesion is the van der Waals force. It has been shown that using the inertia-equivalent approach, the predicted agglomeration rate and the separation efficiency are slightly higher and lower, respectively, compared to the volume-equivalent method (see Figure 7). Furthermore, it is shown that for an inlet mass loading ratio of 0.1 kg_s/kg_g , the difference between the predicted velocity profiles considering two- and four-way coupling methods is small. However, when comparing the predicted grade efficiencies of two- and four-way coupled simulations, as shown in Figure 7, for very small particles, i.e., less than 2 μm in diameter, neglecting the agglomeration may lead to an underprediction of separation efficiency. This is in agreement with the agglomeration concept of Mothes and Löffler [30] regarding particle separation in cyclones, discussed in Section 2.2. The agglomeration effect is also investigated through one-way coupled CFD simulations of gas–solid cyclones [122].

4.3.2. E–E Simulations

E–E studies of gas–solid cyclone separators are very scarce, with the early investigations being allotted to the prediction of the change of cyclone hydrodynamics with the addition of particles [67,123]. In most of the existing E–E studies of gas–solid cyclones, the comparison with experimental data is carried out for cyclones operating with very low particle mass loadings [124–126], i.e., below 0.01 kg_s/kg_g , while the true advantage of using the E–E approach is for the high loading of particles. Costa et al. [126] implemented an E–E simulation of gas–solid flow in a cyclone with four-way coupling. At a solid mass loading of 0.009 kg_s/kg_g , the predicted grade efficiencies were improved by increasing the number of solid phases (corresponding to each size bin), but still overpredicted compared to the experimental data. Variations of this model are further utilized for optimization

studies of gas–solid cyclones operating with either a very low mass loading of particles [127,128] or moderate loadings [129], i.e., $0.1 \text{ kg}_s/\text{kg}_g$, and higher.

For a particle mass loading of around $1 \text{ kg}_s/\text{kg}_g$, mixture models of cyclones are available [130,131], based on modeling the velocity slip between the phases (simplest approach mentioned in Table 1). The pressure drop estimated by these models is underpredicted [130,131], especially at high inlet solids loadings, i.e., $0.4 \text{ kg}_s/\text{kg}_g$, which, according to the authors, is due to the limitation of the granular and mixture models for densely loaded cyclones. Furthermore, the predicted separation efficiencies, compared to the measurements, are not conclusive [130]. In both studies, however, a reduction of swirl by increasing the mass loading is reported.

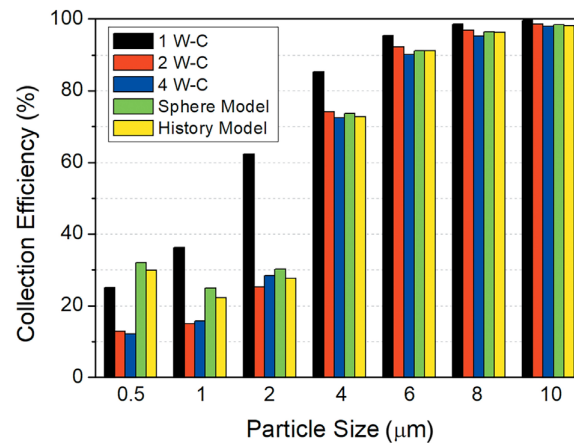


Figure 7. Grade efficiency predicted by the CFD simulation of Sgrott and Sommerfeld [108] for a pilot-scale cyclone loaded with particles with a diameter of 0.5–60 microns and a mass loading of $0.1 \text{ kg}_s/\text{kg}_g$. 1 W-C, 2 W-C, and 4 W-C refer to one-way coupling, two-way coupling, and four-way coupling methods (using CFD–DEM without agglomeration), respectively. Sphere and history models are volume-equivalent and inertia-equivalent approaches for agglomeration, respectively. Reproduced with permission from O.L. Sgrott and M. Sommerfeld, Influence of inter-particle collisions and agglomeration on cyclone performance and collection efficiency; published by John Wiley and Sons, 2018.

4.4. Summary

In this section, the existing CFD simulation studies of reversed-flow cyclone separators operating at ambient temperature are discussed and categorized based on the gas–solid coupling regime of the operating cyclone. For the single-phase gas flow in cyclones, the existing CFD simulation studies are able to accurately capture the velocity and pressure fields as compared to the available experimental data. According to these studies, the RSTM is favorable over other turbulence models with respect to accuracy and computational overhead. However, some modified versions of first-order turbulence models, e.g., $k-\epsilon$ curvature correction (cc) model [66], can still be used in the CFD simulations, especially when the solids loading is high and the swirl is less intense.

For dilute loading of particles and using the one-way coupling method, it is possible to properly capture the separation efficiency of particles in the cyclone as long as the one-way coupling condition is valid for the particle-laden flow. LES has proven to be more accurate in the prediction of grade efficiency, especially for small-sized particles, compared to RSTM, due to an improved prediction of velocity fluctuations and turbulent dispersion.

Among the available gas–solid simulation approaches listed in Table 1, the unresolved E–L and hybrid models are used more frequently, for dilute/medium and dense loading of particles in cyclones, respectively. For densely loaded cyclones, a few CFD studies focus on the effect of solids loading on performance, applying either DDPM–KTGF or CFD–DEM approaches, while only a handful of them investigate the loading of small-sized particles, i.e., 0.1–200 μm in diameter. In the existing CFD studies

of densely loaded cyclones, comparison of the modified flow field with measurements is carried out very rarely, mainly due to challenges in the measurement methods for such systems. Furthermore, comparison/validation of the predicted pressure drops against measurements is usually carried out, rather than the separation efficiency.

5. CFD Simulation Studies of Gas–Solid Cyclones at Elevated Temperatures

In general, the available studies on the CFD simulation of cyclones operating at elevated temperatures are more scarce than the ones for cyclones operating at ambient temperature. Similar to the previous section, the CFD simulations of cyclone separators operating at elevated temperatures can be divided into three groups: single-phase flow, one-way coupled flow, and two/four-way coupled flow simulations. In this section, the three groups of studies are discussed with a focus on the process or physics that is investigated through the CFD simulation.

5.1. Group I: Single-Phase Flow CFD Simulations

Once the operating temperature increases, the physics of gas flow inside the cyclone become more complicated, mainly due to the heat transfer and subsequently variable gas density and viscosity in local regions, if the insulation is not perfect. In turn, since an extra transport equation for energy needs to be solved, the CFD calculation of gas flow becomes computationally more complex and demanding. However, in some of the existing CFD studies of cyclones operating at elevated temperatures, in order to avoid this complexity, the simulations are carried out at a fixed gas temperature, while the gas density and viscosity values are modified according to the operating temperature. Using this method, the predicted pressure drop is reported to be of acceptable accuracy compared to the measurements [131,132].

Similar to the CFD simulations of the cyclones at ambient temperature, accurate modeling of the turbulence is a must to achieve acceptable accuracy for high-temperature single-phase flow simulations of cyclones. However, as mentioned earlier, the increased viscosity as well as decreased density of the carrier gas at elevated temperatures leads to a reduction of swirl intensity and turbulence, indicating the possibility of using a wider range of available turbulence models while keeping the prediction accuracy reasonable. Gimbut et al. [133] have compared the predicted pressure drop of a pilot-scale cyclone with the experimental data of [39] using the RNG $k - \epsilon$ and RSTM. At lower temperatures, i.e., 300–800 K, RSTM is reported to provide a more accurate prediction of the pressure drop compared to the RNG $k - \epsilon$, while in the temperature range of 800–1200 K, the predicted pressure drops using RNG $k - \epsilon$ and RSTM are nearly the same and in agreement with the experimental data [133]. In the existing CFD studies of cyclones operating at elevated temperatures, both the $k - \epsilon$ [134] and RSTM [132] are used as turbulence models.

The tendency for weakened swirl and the modification of the internal velocity field, as an outcome of an elevated operating temperature, is reported in some of the existing CFD studies. According to the CFD simulation results of Shi et al. [132], an overall increase in the axial velocity profiles, weakened reverse flow at the center of the inner vortex, and weakened tangential velocity peaks (weakened swirl), are reported as the operating temperature of the studied pilot-scale cyclone increases from 20 °C to 800 °C. They reported that as the cyclone swirl intensity is weakened at elevated temperatures, the pressure drop is also reduced, and this reduction is dominantly affected by the gas density rather than its viscosity when the volumetric flow rate to the cyclone is kept constant [132]. The reduction of pressure drop with the gas temperature is reported in many of the existing CFD studies of cyclones operating at elevated temperatures [41,132,134–136]. An approach for the comprehensive analysis of local energy loss in cyclones is through evaluating entropy generation in CFD simulation, which has been carried out for cyclones operating at ambient [137,138] and elevated [135] temperatures. Duan et al. [135] have numerically investigated entropy generation in a cyclone system operating in a temperature range of 297–1123 K. According to this study, turbulence dissipation and wall friction are the main contributors to the energy loss. The ratio of contribution of both parameters is

nearly unaffected by the gas temperature, whereas their magnitude decreases at higher operating temperatures due to the reduction in gas density. The maximum energy loss takes place in areas close to the vortex finder and the entrance of the dust bin.

5.2. Group II: One-Way Coupled Gas–Solid Flow Simulations

In the existing CFD studies of cyclones operating at elevated temperatures, the predicted separation efficiency is negatively affected by the temperature. Gimbun [41] has performed one-way coupled simulations of a pilot-scale cyclone using RSTM and a stochastic tracking of particles in a temperature range of 20–900 °C. For a fixed inlet gas velocity, the predicted grade separation efficiencies and particle cut-sizes were in proper agreement with the experimental data, and overall, the separation efficiency worsened with the temperature. The reduction in separation efficiency was stated to be a direct consequence of the weakened centrifugal effect. In the same line of research, Gimbun et al. [139] presented an accurate prediction of the particle cut-size for different cyclone types compared to experiments, at ambient and elevated temperatures. The reduction of separation efficiency is also reported in some of other studies (for example, see [134,136]).

One-way coupled heat transfer to solids particles fed in to a pilot-scale cyclone was studied by Mothilal and Pitchandi [140,141] using E–L simulation and RNG $k - \epsilon$ turbulence models and at an inlet air temperature of 200 °C. The predicted pressure drop was compared with the available experimental data for the particle-free case, while for the gas–solid cases, no validation was presented. By increasing the gas velocity at the cyclone inlet, the centrifugal effect on particles was improved and the predicted particle hold-up in the system was increased, especially for larger mass loadings of particles. This leads to a greater available surface area (for heat transfer) as well as a higher residence time of particles in the cyclone system.

5.3. Group III: Two- and Four-Way Coupled Gas–Solid Flow Simulations

In this group of studies, both E–L and E–E and hybrid approaches are applied for the CFD simulation of cyclones operating at elevated temperatures; these are discussed here with a focus on the studies that have investigated the performance of industrial-scale cyclones.

5.3.1. Cyclone Heat Exchangers

An important industrial application of cyclones is the solids preheating process used in, e.g., cement industry. The performance evaluation for full-scale cyclone heat exchangers is carried out in some of the existing studies and summarized in Table 3. Cristea and Conti [142,143] have applied a DDPM–KTGF approach to simulate the gas–solid flow in the preheater system (excluding the calciner) of a cement factory with an approximate height of 58 m. The gas–solid heat transfer as well as the calcination reaction are included in the CFD model [143]. As compared to the industrial measurements for the first-stage twin cyclones, the predicted pressure drop and separation efficiencies are in good agreement with the measurements, while the exit gas temperature is overpredicted. This discrepancy has been attributed to the complications that arise with the modeling of the high mass loading of particles in the upper-stage calciner [143]. Mikulčić et al. [144] have conducted a two-way coupled CFD simulation study of an industrial-scale cyclone belonging to the preheater system of a dry kiln process. The simulations aimed to assess the gas–solid heat transfer as well as the progress of the calcination process in the studied cyclone. The predicted pressure drop was in fair agreement with the measurements, while the outlet gas temperature was slightly overpredicted, and the authors did not provide any reasoning for this mismatch. In this CFD study, low gas temperature regions in the upper part of the cyclone and close to the walls were observed, due to the endothermic calcination reaction. Wasilewski [145] conducted a two-way coupled CFD simulation of a full-scale cyclone preheater and reported a reduction of the separation efficiency with increased temperatures and decreased particle loading. However, as compared to the measurements, an underprediction of the separation efficiencies is reported, which is claimed to be due to the limitation of the CFD model in taking into account the

particle–particle interactions, i.e., collision and agglomeration. Presented in Figure 8 is their predicted trajectories and heat-transfer rate to laden particles of different diameters. The smaller-sized particles have a higher tendency to travel through the central regions of the cyclone body and escape from the vortex finder. In addition, they have a higher rate of heat exchange with the gas, especially at regions close to the inlet, compared to the larger-sized particles. In contrast, larger-sized particles have a higher tendency to travel in spiral clouds along the cyclone walls and toward the particle exit chamber.

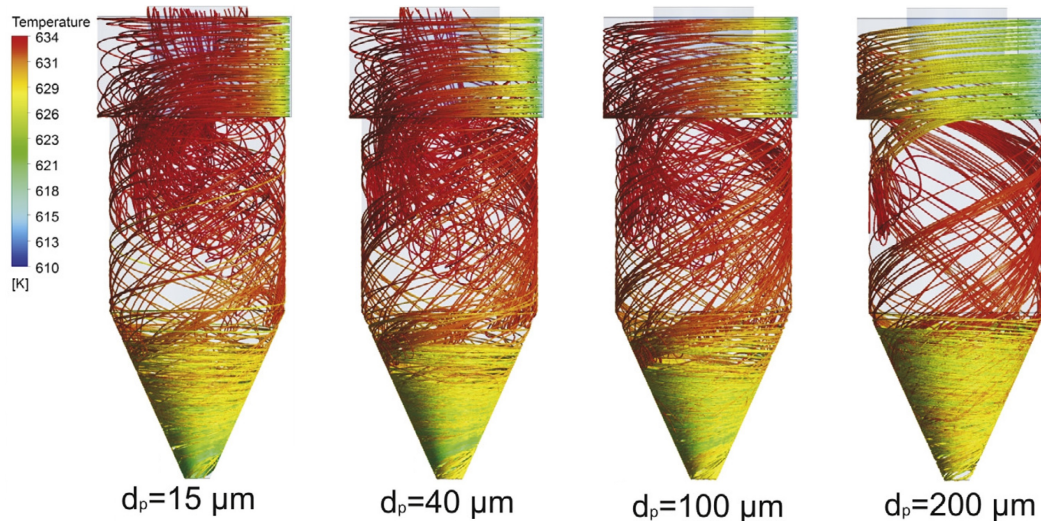


Figure 8. Predicted trajectories of particles of different diameters in an industrial-scale cyclone with a body diameter of 3.45 m. The trajectories are colored with particle temperature. The inlet gas and particle temperatures are 634 K and 611 K, respectively, and inlet solids mass loading is around 0.8 kg_s/kg_g [145]. Reproduced with permission from M. Wasilewski, Analysis of the effects of temperature and the share of solid and gas phases on the process of separation in a cyclone suspension preheater; published by Elsevier, 2016.

Table 3. Selected CFD studies of industrial-scale cyclones operating at elevated temperatures, in chronological order.

Author(s)	Scale of Simulation	CFD Solver	Gas–Solid Model	Turbulence/Drag Models
Cristea and Conti [143]	Preheater system (\approx 58 m height)	ANSYS FLUENT 18.1	hybrid (DDPM–KTGF)	RSTM/Schiller and Naumann [146]
Mikulčić et al. [144]	Industrial cyclone (\approx 13 m height and 6 m diameter)	FIRE commercial solver	E–L (two–way coupled)	LES/not mentioned
Wasilewski [145]	Industrial cyclone (\approx 9 m height and 3.5 m diameter)	ANSYS FLUENT 14	E–L (two–way coupled)	RSTM/Schiller and Naumann [146]

There are also a few E–E simulation studies of cyclones at elevated temperatures. In the study of Vegini et al. [124], 2D axisymmetric simulations of full-scale cyclone separators connected in series and operating at elevated temperature were carried out. The selected turbulence model is a combination of the standard $k - \epsilon$ and Prandtl’s longitudinal mixing model, which is claimed to be accurate enough for capturing the anisotropic effect of Reynolds stress in swirling turbulent flows. The numerical model was validated against the available grade efficiencies and pressure drops at ambient temperature and a dust load of around 0.004 kg_s/kg_g. In elevated temperature conditions, the predicted pressure drop values were generally overpredicted compared to the available long-term full-scale measurements. This overprediction was claimed to be due to the presence of false air in the system, and as a consequence, a reduction of swirl. The presence of false air is not considered in the simulations.

5.3.2. CFD Simulation of Cyclones as a Part of a Bigger System

There are a number of studies that have carried out CFD simulations of elevated-temperature cyclones as a part of a bigger process system, e.g., a circulating fluidized bed (CFB) boiler. An important phenomenon that is explored in this type of study is the fluctuation and maldistribution of gas and solid flows at the inlet of parallel cyclones, which can, in turn, affect cyclone performance. The subject is investigated both experimentally [147–150] and numerically [151,152]. Zhang et al. [151] have reported temporal synchronized fluctuations of solid flux at the inlet of two parallel cyclones based on four-way coupled E–E simulations of a 150 MW CFB boiler operating at 917 °C. Jiang et al. [152] have carried out hybrid E–L and E–L (MP–PIC) CFD simulations of a scaled down circulating fluidized bed comprised of six parallel cyclones. They reported a non-uniformity in the average solid concentration downstream of the cyclone diplegs, based on both simulations and experimental data. However, some of the predicted solid concentrations were somewhat different from those of the measurements, with the highest relative error being around 28%.

5.4. Summary

The existing CFD studies of cyclones operating at elevated temperatures were discussed in this section, with a focus on the ones investigating cyclone performance parameters, i.e., pressure drop, separation efficiency, and gas–solid heat transfer. The gas-flow simulation studies reveal that CFD simulations are capable of capturing the reduced swirl intensity and reduced pressure drop as a result of elevated temperature. Furthermore, in some of the studies, the first-order turbulence models are satisfactorily used to calculate the gas flow field. The reduction in separation efficiency of dilutely loaded cyclones, i.e., one-way coupled studies, due to the increase in temperature, is captured. A number of CFD studies of industrial-scale cyclones are also described. However, it is common for the full-scale measurements of these systems not to exist or to be limited, e.g., to only the pressure drop of the cyclone for a specific operating condition, indicating the lack of complete validation of the accuracy of current CFD studies.

6. Outlook

In this review, the capability of computational fluid dynamics in predicting the gas–solid flow field and performance of cyclone separators, operating at dilute–high loading of particles and ambient and elevated temperatures, is discussed. Summaries of ambient- and elevated-temperature CFD studies are provided in Sections 4.4 and 5.4. In general, it can be stated that the CFD simulation can be used as a powerful tool to successfully predict the flow field and performance of cyclone separators, i.e., pressure drop and separation efficiency, with the E–L and hybrid methods being the most frequently used approaches. However, as the mass loading and the operating temperature increase, the validation of the internal flow field, which is important for a better understanding of the separation process, becomes challenging due to the lack of experimental data. For these cyclones, the validation is so far limited to the comparison of the pressure drop and seldom the measured separation efficiency.

The drag models that are usually applied in two- and four-way coupled simulations are well-known homogeneous models, e.g., Wen–Yu [113] and Gidaspow [50], while heterogeneous models, e.g., the energy-minimization-multi-scale (EMMS) approach [153], are rarely used (for example, see [111]). In the authors' opinion, heterogeneous drag models can be more suitable for CFD simulation of heavily loaded cyclones (e.g., inlet mass loading on the order of 1–100 kg_s/kg_g), as it is likely to have cluster formation in the internal regions, apart from regions close to the cyclone walls, especially for the elevated operating temperatures with weakened centrifugal effect.

Author Contributions: Conceptualization, M.N. and H.W.; investigation, M.N.; writing—original draft preparation, M.N.; writing—review and editing, M.N.; supervision, H.W., B.L., Y.T., W.W., K.D.-J.; project administration, H.W.; funding acquisition, H.W., K.D.-J. All authors have read and agreed to the published version of the manuscript.

Funding: This project is supported by the Sino-Danish Centre for Education and Research; and the ProBu - Process Technology for Sustainable Building Materials Production - project (grant number: 8055-00014B) funded by Innovation Fund Denmark, FLSmith A/S, Rockwool International A/S and Technical University of Denmark.

Conflicts of Interest: The authors declare no conflict of interest.

Abbreviations

The following abbreviations are used in this manuscript:

CFB	Circulating fluidized bed
CFD	Computational fluid dynamics
DDPM	Dense discrete phase model
DEM	Discrete element method
DRW	Discrete random walk
E-E	Eulerian–Eulerian
E-L	Eulerian–Lagrangian
LES	Large eddy simulation
LRR	Lauder, Reece, and Rodi model [73] (variation of the RSTM)
KTGF	Kinetic theory of granular flows
PBM	Population balance model
PVC	Precessing vortex core
RSTM	Reynolds stress transport model
SGS	Subgrid-scale
SSG	Speziale, Sarkar, and Gatski model [74] (variation of the RSTM)
UDF	User-defined function
URANS	Unsteady Reynolds-averaged Navier–Stokes

References

- Jain, A.; Mohanty, B.; Pitchumani, B.; Rajan, K. Studies on Gas-Solid Heat Transfer in Cyclone Heat Exchanger. *J. Heat Transf.* **2006**, *128*, 761. [[CrossRef](#)]
- He, P.; Luo, S.; Cheng, G.; Xiao, B.; Cai, L.; Wang, J. Gasification of biomass char with air-steam in a cyclone furnace. *Renew. Energy* **2012**, *37*, 398–402. [[CrossRef](#)]
- Barnhart, J.; Laurendeau, N. Pulverized coal combustion and gasification in a cyclone reactor. 1. Experiment. *Ind. Eng. Chem. Process Des. Dev.* **1982**, *21*, 671–680. [[CrossRef](#)]
- Zhen, F. A biomass pyrolysis gasifier applicable to rural China. *Fuel Sci. Technol. Int.* **1993**, *11*, 1025–1035. [[CrossRef](#)]
- Green, N.W.; Duraiswamy, K.; Lumpkin, R.E. Pyrolysis with Cyclone Burner. U.S. Patent 4102773A, 25 July 1978.
- Muschelknautz, U.; Muschelknautz, E. *Separation Efficiency of Recirculating Cyclones in Circulating Fluidized Bed Combustions*; VGB PowerTech: Essen, Germany, 1999; Volume 79, pp. 48–53.
- Hoffmann, A.; van Santen, A.; Allen, R.; Clift, R. Effects of geometry and solid loading on the performance of gas cyclones. *Powder Technol.* **1992**, *70*, 83–91. [[CrossRef](#)]
- Muschelknautz, E.; Brunner, K. Untersuchungen an Zyklonen. *Chemie Ing. Tech.* **1967**, *39*, 531–538. [[CrossRef](#)]
- Yuu, S.; Jotaki, T.; Tomita, Y.; Yoshida, K. The reduction of pressure drop due to dust loading in a conventional cyclone. *Chem. Eng. Sci.* **1978**, *33*, 1573–1580. [[CrossRef](#)]
- Kang, S.; Kwon, T.; Kim, S. Hydrodynamic characteristics of cyclone reactors. *Powder Technol.* **1989**, *58*, 211–220. [[CrossRef](#)]
- Alexander, R. Fundamentals of cyclone design and operation. *Proc. Australas Inst. Min. Met.* **1949**, *152*, 202.
- Barth, W. Berechnung und Auslegung von Zyklonabscheidern auf Grund neuerer Untersuchungen. *Brennst-Waerme-Kraft* **1956**, *8*, 1–9.
- Muschelknautz, E. Die Berechnung von Zyklonabscheidern für Gase. *Chemie Ing. Tech.* **1972**, *44*, 63–71. [[CrossRef](#)]
- Meißner, P.; Löffler, F. Zur Berechnung des Strömungsfeldes im Zyklonabscheider. *Chemie Ing. Tech.* **1978**, *50*, 471. [[CrossRef](#)]
- Reydon, R.; Gauvin, W. Theoretical and experimental studies of confined vortex flow. *Can. J. Chem. Eng.* **1981**, *59*, 14–23. [[CrossRef](#)]

16. Muschelknautz, E.; Krambrock, W. Aerodynamische Beiwerte des Zyklonabscheiders aufgrund neuer und verbesserter Messungen. *Chem. Ing. Tech.* **1970**, *42*, 247–255. [[CrossRef](#)]
17. Hsiao, T.; Chen, D.; Greenberg, P.; Street, K. Effect of geometric configuration on the collection efficiency of axial flow cyclones. *J. Aerosol Sci.* **2011**, *42*, 78–86. [[CrossRef](#)]
18. Xiong, Z.; Ji, Z.; Wu, X. Development of a cyclone separator with high efficiency and low pressure drop in axial inlet cyclones. *Powder Technol.* **2014**, *253*, 644–649. [[CrossRef](#)]
19. Hoffmann, A.; Stein, L. *Gas Cyclones and Swirl Tubes*; Springer: Berlin/Heidelberg, Germany, 2007; pp. 1–422. [[CrossRef](#)]
20. Cortés, C.; Gil, A. Modeling the gas and particle flow inside cyclone separators. *Prog. Energy Combust. Sci.* **2007**, *33*, 409–452. [[CrossRef](#)]
21. Towler, G.; Sinnott, R. Specification and design of solids-handling equipment. *Chem. Eng. Des.* **2013**, *937*–1046. [[CrossRef](#)]
22. Trefz, M.; Muschelknautz, E. Extended cyclone theory for gas flows with high solids concentrations. *Chem. Eng. Technol.* **1993**, *16*, 153–160. [[CrossRef](#)]
23. ter Linden, A. Investigations into Cyclone Dust Collectors. *Proc. Inst. Mech. Eng.* **1949**, *160*, 233–251. [[CrossRef](#)]
24. Majumder, A.; Shah, H.; Shukla, P.; Barnwal, J. Effect of operating variables on shape of “fish-hook” curves in cyclones. *Miner. Eng.* **2007**, *20*, 204–206. [[CrossRef](#)]
25. Haig, C.; Hursthouse, A.; McIlwain, S.; Sykes, D. The effect of particle agglomeration and attrition on the separation efficiency of a Stairmand cyclone. *Powder Technol.* **2014**, *258*, 110–124. [[CrossRef](#)]
26. Barth, W. Design and Layout of the Cyclone Separator on the Basis of New Investigations. *Brennstow-Wärme-Kraft (BWK)* **1956**, *8*, 1–9.
27. Hugi, E.; Reh, L. Focus on solids strand formation improves separation performance of highly loaded circulating fluidized bed recycle cyclones. *Chem. Eng. Process. Process Intensif.* **2000**, *39*, 263–273. [[CrossRef](#)]
28. Hoffmann, A.; Arends, H.; Sie, H. An experimental investigation elucidating the nature of the effect of solids loading on cyclone performance. *Filtr. Sep.* **1991**, *28*, 188–193. [[CrossRef](#)]
29. Fassani, F.; Goldstein, L. A study of the effect of high inlet solids loading on a cyclone separator pressure drop and collection efficiency. *Powder Technol.* **2000**, *107*, 60–65. [[CrossRef](#)]
30. Mothes, H.; Löffler, F. Motion and deposition of particles in cyclones. *Ger. Chem. Eng.* **1985**, *8*, 223–233.
31. Comas, M.; Comas, J.; Chetrit, C.; Casal, J. Cyclone pressure drop and efficiency with and without an inlet vane. *Powder Technol.* **1991**, *66*, 143–148. [[CrossRef](#)]
32. Baskakov, A.; Dolgov, V.; Goldobin, Y. Aerodynamics and heat transfer in cyclones with particle-laden gas flow. *Exp. Therm. Fluid Sci.* **1990**, *3*, 597–602. [[CrossRef](#)]
33. Huang, Y.; Mo, X.; Yang, H.; Zhang, M.; Lv, J. Effects of Cyclone Structures on the Pressure Drop Across Different Sections in Cyclone Under Gas-Solid Flow. In *Clean Coal Technology and Sustainable Development*; Springer: Singapore, 2016; pp. 301–307. [[CrossRef](#)]
34. Ashry, E.; Abdelrazek, A.; Elshorbagy, K. Numerical and experimental study on the effect of solid particle sphericity on cyclone pressure drop. *Sep. Sci. Technol.* **2018**, *53*, 2500–2516. [[CrossRef](#)]
35. Hwang, I.; Jeong, H.; Hwang, J. Numerical simulation of a dense flow cyclone using the kinetic theory of granular flow in a dense discrete phase model. *Powder Technol.* **2019**, *356*, 129–138. [[CrossRef](#)]
36. Li, S.; Yang, H.; Wu, Y.; Zhang, H. An Improved Cyclone Pressure Drop Model at High Inlet Solid Concentrations. *Chem. Eng. Technol.* **2011**, *34*, 1507–1513. [[CrossRef](#)]
37. Wu, X.; Liu, J.; Xu, X.; Xiao, Y. Modeling and experimental validation on pressure drop in a reverse-flow cyclone separator at high inlet solid loading. *J. Therm. Sci.* **2011**, *20*, 343–348. [[CrossRef](#)]
38. Dewil, R.; Baeyens, J.; Caerts, B. CFB cyclones at high temperature: Operational results and design assessment. *Particulology* **2008**, *6*, 149–156. [[CrossRef](#)]
39. Bohnet, M. Influence of the gas temperature on the separation efficiency of aerocyclones. *Chem. Eng. Process. Process Intensif.* **1995**, *34*, 151–156. [[CrossRef](#)]
40. Patterson, P.; Munz, R. Cyclone collection efficiencies at very high temperatures. *Can. J. Chem. Eng.* **1989**, *67*, 321–328. [[CrossRef](#)]
41. Gimbut, J. CFD Simulation of Aerocyclone Hydrodynamics and Performance at Extreme Temperature. *Eng. Appl. Comput. Fluid Mech.* **2008**, *2*, 22–29. [[CrossRef](#)]
42. Szekely, J.; Carr, R. Heat transfer in a cyclone. *Chem. Eng. Sci.* **1966**, *21*, 1119–1132. [[CrossRef](#)]

43. Danyluk, S.; Shack, W.; Park, J.; Mamoun, M. The erosion of a Type 310 stainless steel cyclone from a coal gasification pilot plant. *Wear* **1980**, *63*, 95–104. [[CrossRef](#)]
44. Chen, Y.; Nieskens, M.; Karri, S.; Knowlton, T. Developments in cyclone technology improve FCC unit reliability. *Pet. Technol. Q.* **2010**, *15*, 65–71.
45. Kim, S.; Lee, J.; Kim, C.; Koh, J.; Kim, G.; Choi, S. Characteristics of Deposits Formed in Cyclones in Commercial RFCC Reactor. *Ind. Eng. Chem. Res.* **2012**, *51*, 10238–10246. [[CrossRef](#)]
46. Kim, S.; Lee, J.; Koh, J.; Kim, G.; Choi, S.; Yoo, I. Formation and Characterization of Deposits in Cyclone Dipleg of a Commercial Residue Fluid Catalytic Cracking Reactor. *Ind. Eng. Chem. Res.* **2012**, *51*, 14279–14288. [[CrossRef](#)]
47. Yoshida, H.; Fukui, K.; Yoshida, K.; Shinoda, E. Particle separation by Inoya's type gas cyclone. *Powder Technol.* **2001**, *118*, 16–23. [[CrossRef](#)]
48. van der Hoef, M.; van Sint Annaland, M.; Deen, N.; Kuipers, J. Numerical Simulation of Dense Gas-Solid Fluidized Beds: A Multiscale Modeling Strategy. *Annu. Rev. Fluid Mech.* **2008**, *40*, 47–70. [[CrossRef](#)]
49. Fan, L.; Zhu, C. *Principles of Gas-Solid Flows*; Cambridge Series in Chemical Engineering; Cambridge University Press: Cambridge, UK, 1998.
50. Gidaspow, D. *Multiphase Flow and Fluidization: Continuum and Kinetic Theory Descriptions*; Academic Press: Cambridge, MA, USA, 1994; p. 467.
51. Zeneli, M.; Nikolopoulos, A.; Nikolopoulos, N.; Grammelis, P.; Karellas, S.; Kakaras, E. Simulation of the reacting flow within a pilot scale calciner by means of a three phase TFM model. *Fuel Process. Technol.* **2017**, *162*, 105–125. [[CrossRef](#)]
52. Mathiesen, V.; Solberg, T.; Hjertager, B. Predictions of gas-particle flow with an Eulerian model including a realistic particle size distribution. *Powder Technol.* **2000**, *112*, 34–45. [[CrossRef](#)]
53. Rizk, M.A. Mathematical modeling of densely loaded, particle-laden turbulent flows. *Automization Sprays* **1993**, *3*, 1–27.
54. Ibsen, C.; Helland, E.; Hjertager, B.; Solberg, T.; Tadrst, L.; Occelli, R. Comparison of multifluid and discrete particle modelling in numerical predictions of gas particle flow in circulating fluidised beds. *Powder Technol.* **2004**, *149*, 29–41. [[CrossRef](#)]
55. Cundall, P.; Strack, O. A discrete numerical model for granular assemblies. *Géotechnique* **1979**, *29*, 47–65. [[CrossRef](#)]
56. Andrews, M.; O'Rourke, P. The multiphase particle-in-cell (MP-PIC) method for dense particulate flows. *Int. J. Multiph. Flow* **1996**, *22*, 379–402. [[CrossRef](#)]
57. Snider, D.; O'Rourke, P. The multiphase particle-in-cell (MP-PIC) method for dense particle flow. *Int. J. Multiph. Flow* **2010**, *22*, 277–314. [[CrossRef](#)]
58. Andrews, M.; Baillergeau, D.; O'Rourke, P. A Lagrangian particle method for the simulation of dense particulate flows. *Am. Soc. Mech. Eng. Fluids Eng. Div.* **1994**, *199*, 37–46.
59. Popoff, B.; Braun, M. A Lagrangian Approach to Dense Particulate Flows. In Proceedings of the ICMF 2007 6th International Conference on Multiphase Flow, Leipzig, Germany, 9–13 July 2007; p. 11.
60. van der Hoef, M.; Ye, M.; van Sint Annaland, M.; Andrews, A.; Sundaresan, S.; Kuipers, J. Multiscale modeling of gas-fluidized beds. *Adv. Chem. Eng.* **2006**, *31*, 65–149. [[CrossRef](#)]
61. Elghobashi, S. On predicting particle-laden turbulent flows. *Appl. Sci. Res.* **1994**, *52*, 309–329. [[CrossRef](#)]
62. Hamdy, O.; Bassily, M.; El-Batsh, H.; Mekhail, T. Numerical study of the effect of changing the cyclone cone length on the gas flow field. *Appl. Math. Model.* **2017**, *46*, 81–97. [[CrossRef](#)]
63. Hoekstra, A.; Derksen, J.; Van Den Akker, H. An experimental and numerical study of turbulent swirling flow in gas cyclones. *Chem. Eng. Sci.* **1999**, *54*, 2055–2065. [[CrossRef](#)]
64. Vaitiekūnas, P.; Jakštonienė, I. Analysis of numerical modelling of turbulence in a conical reverse-flow cyclone. *J. Environ. Eng. Landsc. Manag.* **2010**, *18*, 321–328. [[CrossRef](#)]
65. Kaya, F.; Karagoz, I. Performance analysis of numerical schemes in highly swirling turbulent flows in cyclones. *Curr. Sci.* **2008**, *94*, 1273–1278.
66. Grotjans, H. Application of higher order turbulence models to cyclone flows. *VDI Berichte* **1999**, *1511*, 175–182.
67. Meier, H.; Mori, M. Anisotropic behavior of the Reynolds stress in gas and gas-solid flows in cyclones. *Powder Technol.* **1999**, *101*, 108–119. [[CrossRef](#)]

68. Qian, F.; Zhang, J.; Zhang, M. Effects of the prolonged vertical tube on the separation performance of a cyclone. *J. Hazard. Mater.* **2006**, *136*, 822–829. [[CrossRef](#)] [[PubMed](#)]
69. Wang, B.; Xu, D.; Chu, K.; Yu, A. Numerical study of gas-solid flow in a cyclone separator. *Appl. Math. Model.* **2006**, *30*, 1326–1342. [[CrossRef](#)]
70. Afolabi, L.; Aroussi, A.; Isa, N. Numerical modelling of the carrier gas phase in a laboratory-scale coal classifier model. *Fuel Process. Technol.* **2011**, *92*, 556–562. [[CrossRef](#)]
71. Derksen, J.; Van den Akker, H. Simulation of vortex core precession in a reverse-flow cyclone. *AIChE J.* **2000**, *46*, 1317–1331. [[CrossRef](#)]
72. Derksen, J. Simulations of confined turbulent vortex flow. *Comput. Fluids* **2005**, *34*, 301–318. [[CrossRef](#)]
73. Launder, B.; Reece, G.; Rodi, W. Progress in the development of a Reynolds-stress turbulence closure. *J. Fluid Mech.* **1975**, *68*, 537. [[CrossRef](#)]
74. Speziale, C.; Sarkar, S.; Gatski, T. Modelling the pressure-strain correlation of turbulence: An invariant dynamical systems approach. *J. Fluid Mech.* **1991**, *227*, 245–272. [[CrossRef](#)]
75. Elsayed, K.; Lacor, C. Analysis and Optimisation of Cyclone Separators Geometry Using RANS and LES Methodologies. In *Turbulence and Interactions. Notes on Numerical Fluid Mechanics and Multidisciplinary Design*; Deville, M., Estivalezes, J.L., Gleize, V., Lê, T.H., Terracol, M., Vincent, S., Eds.; Springer, Berlin/Heidelberg, Germany, 2014; pp. 65–74. [[CrossRef](#)]
76. Gronald, G.; Derksen, J. Simulating turbulent swirling flow in a gas cyclone: A comparison of various modeling approaches. *Powder Technol.* **2011**, *205*, 160–171. [[CrossRef](#)]
77. Jang, K.; Lee, G.; Huh, K. Evaluation of the turbulence models for gas flow and particle transport in URANS and LES of a cyclone separator. *Comput. Fluids* **2018**, *172*, 274–283. [[CrossRef](#)]
78. Shukla, S.; Shukla, P.; Ghosh, P. Evaluation of numerical schemes using different simulation methods for the continuous phase modeling of cyclone separators. *Adv. Powder Technol.* **2011**, *22*, 209–219. [[CrossRef](#)]
79. Derksen, J. Separation performance predictions of a Stairmand high-efficiency cyclone. *AIChE J.* **2003**, *49*, 1359–1371. [[CrossRef](#)]
80. Kępa, A. The influence of a plate vortex limiter on cyclone separator. *Sep. Sci. Technol.* **2016**, *51*, 1–13. [[CrossRef](#)]
81. Song, C.; Pei, B.; Jiang, M.; Wang, B.; Xu, D.; Chen, Y. Numerical analysis of forces exerted on particles in cyclone separators. *Powder Technol.* **2016**, *294*, 437–448. [[CrossRef](#)]
82. Guo, Q.; Wang, Q.; Lu, X.; Ji, P.; Kang, Y. Numerical Simulation for a CFB Boiler's Cyclone Separator with Structure Optimizations. In *Clean Coal Technology and Sustainable Development*; Springer: Singapore, 2016; pp. 257–263. [[CrossRef](#)]
83. Haig, C.; Hursthouse, A.; Sykes, D.; McIlwain, S. The rapid development of small scale cyclones - numerical modelling versus empirical models. *Appl. Math. Model.* **2016**, *40*, 6082–6104. [[CrossRef](#)]
84. Amirante, R.; Tamburrano, P. Tangential inlet cyclone separators with low solid loading. *Eng. Comput.* **2016**, *33*, 2090–2116. [[CrossRef](#)]
85. Sun, X.; Zhang, Z.; Chen, D. Numerical modeling of miniature cyclone. *Powder Technol.* **2017**, *320*, 325–339. [[CrossRef](#)]
86. Zhang, G.; Chen, G.; Yan, X. Evaluation and improvement of particle collection efficiency and pressure drop of cyclones by redistribution of dustbins. *Chem. Eng. Res. Des.* **2018**, *139*, 52–61. [[CrossRef](#)]
87. Mazyan, W.; Ahmadi, A.; Brinkerhoff, J.; Ahmed, H.; Hoorfar, M. Enhancement of cyclone solid particle separation performance based on geometrical modification: Numerical analysis. *Sep. Purif. Technol.* **2018**, *191*, 276–285. [[CrossRef](#)]
88. Elsayed, K.; Lacor, C. Numerical modeling of the flow field and performance in cyclones of different cone-tip diameters. *Comput. Fluids* **2011**, *51*, 48–59. [[CrossRef](#)]
89. de Souza, F.; de Vasconcelos Salvo, R.; de Moro Martins, D. Large Eddy Simulation of the gas-particle flow in cyclone separators. *Sep. Purif. Technol.* **2012**, *94*, 61–70. [[CrossRef](#)]
90. Misiulia, D.; Andersson, A.; Lundström, T. Computational Investigation of an Industrial Cyclone Separator with Helical-Roof Inlet. *Chem. Eng. Technol.* **2015**, *38*, 1425–1434. [[CrossRef](#)]
91. Akiyama, O.; Kato, C. Numerical Investigations of Unsteady Flows and Particle Behavior in a Cyclone Separator. *J. Fluids Eng.* **2017**, *139*, 091302. [[CrossRef](#)]

92. Yohana, E.; Tauviquirrahman, M.; Putra, A.R.; Diana, A.E.; Choi, K.H. Numerical analysis on the effect of the vortex finder diameter and the length of vortex limiter on the flow field and particle collection in a new cyclone separator. *Cogent Eng.* **2018**, *5*. [[CrossRef](#)]
93. Wasilewski, M.; Anweiler, S.; Masiukiewicz, M. Characterization of multiphase gas-solid flow and accuracy of turbulence models for lower stage cyclones used in suspension preheaters. *Chin. J. Chem. Eng.* **2018**. [[CrossRef](#)]
94. Lessani, B.; Nakhaei, M. Large-eddy simulation of particle-laden turbulent flow with heat transfer. *Int. J. Heat Mass Transf.* **2013**, *67*, 974–983. [[CrossRef](#)]
95. Berlemont, A.; Desjonqueres, P.; Gouesbet, G. Particle lagrangian simulation in turbulent flows. *Int. J. Multiph. Flow* **1990**, *16*, 19–34. [[CrossRef](#)]
96. Shukla, S.; Shukla, P.; Ghosh, P. The effect of modeling of velocity fluctuations on prediction of collection efficiency of cyclone separators. *Appl. Math. Model.* **2013**, *37*, 5774–5789. [[CrossRef](#)]
97. Zhao, B. Development of a new method for evaluating cyclone efficiency. *Chem. Eng. Process. Process Intensif.* **2005**, *44*, 447–451. [[CrossRef](#)]
98. Zhou, F.; Sun, G.; Han, X.; Zhang, Y.; Bi, W. Experimental and CFD study on effects of spiral guide vanes on cyclone performance. *Adv. Powder Technol.* **2018**, *29*, 3394–3403. [[CrossRef](#)]
99. Derksen, J.; van den Akker, H.; Sundaresan, S. Two-way coupled large-eddy simulations of the gas-solid flow in cyclone separators. *AIChE J.* **2008**, *54*, 872–885. [[CrossRef](#)]
100. Li, G.; Lu, Y. Cyclone separation in a supercritical water circulating fluidized bed reactor for coal/biomass gasification: Structural design and numerical analysis. *Particuology* **2018**, *39*, 55–67. [[CrossRef](#)]
101. Huang, A.; Ito, K.; Fukasawa, T.; Fukui, K.; Kuo, H. Effects of particle mass loading on the hydrodynamics and separation efficiency of a cyclone separator. *J. Taiwan Inst. Chem. Eng.* **2018**, *90*, 61–67. [[CrossRef](#)]
102. Liu, S.; Guo, Y.; Sun, G.; Weng, L. Flow Simulation and Performance Comparison of Rough-Cut Cyclones with Different Structures in Dilute Phase. *Chem. Eng. Technol.* **2015**, *38*, 1809–1816. [[CrossRef](#)]
103. Tamjid, S.; Hashemabadi, S.; Shirvani, M. Prediction of catalyst attrition in a regeneration cyclone. *Filtr. Sep.* **2010**, *47*, 29–33. [[CrossRef](#)]
104. Cui, J.; Chen, X.; Gong, X.; Yu, G. Numerical Study of Gas-Solid Flow in a Radial-Inlet Structure Cyclone Separator. *Ind. Eng. Chem. Res.* **2010**, *49*, 5450–5460. [[CrossRef](#)]
105. Wan, G.; Sun, G.; Xue, X.; Shi, M. Solids concentration simulation of different size particles in a cyclone separator. *Powder Technol.* **2008**, *183*, 94–104. [[CrossRef](#)]
106. Kozolub, P.; Klimanek, A.; Białecki, R.; Adamczyk, W. Numerical simulation of a dense solid particle flow inside a cyclone separator using the hybrid Euler-Lagrange approach. *Particuology* **2017**, *31*, 170–180. [[CrossRef](#)]
107. Zhou, H.; Hu, Z.; Zhang, Q.; Wang, Q.; Lv, X. Numerical study on gas-solid flow characteristics of ultra-light particles in a cyclone separator. *Powder Technol.* **2019**, *344*, 784–796. [[CrossRef](#)]
108. Sgrott, O.; Sommerfeld, M. Influence of inter-particle collisions and agglomeration on cyclone performance and collection efficiency. *Can. J. Chem. Eng.* **2019**, *97*, 511–522. [[CrossRef](#)]
109. Chu, K.; Wang, B.; Xu, D.; Chen, Y.; Yu, A. CFD-DEM simulation of the gas-solid flow in a cyclone separator. *Chem. Eng. Sci.* **2011**, *66*, 834–847. [[CrossRef](#)]
110. Schneiderbauer, S.; Haider, M.; Hauzenberger, F.; Pirker, S. A Lagrangian-Eulerian hybrid model for the simulation of industrial-scale gas-solid cyclones. *Powder Technol.* **2016**, *304*, 229–240. [[CrossRef](#)]
111. Schneiderbauer, S.; Pirker, S. Filtered and heterogeneity-based subgrid modifications for gas-solid drag and solid stresses in bubbling fluidized beds. *AIChE J.* **2014**, *60*, 839–854. [[CrossRef](#)]
112. Wei, J.; Zhang, H.; Wang, Y.; Wen, Z.; Yao, B.; Dong, J. The gas-solid flow characteristics of cyclones. *Powder Technol.* **2017**, *308*, 178–192. [[CrossRef](#)]
113. Wen, C.; Yu, Y. Mechanics of fluidization. *Chem. Eng. Progress, Symp. Ser.* **1966**, *62*, 100–111.
114. Hoekstra, A. Gas fLow Field and Collection Efficiency of Cyclone Separators. Ph.D. Thesis, Delft University of Technology, Delft, The Netherlands, 2000.
115. Wasilewski, M.; Duda, J. Multicriteria optimisation of first-stage cyclones in the clinker burning system by means of numerical modelling and experimental research. *Powder Technol.* **2016**, *289*, 143–158. [[CrossRef](#)]
116. Derksen, J.; Sundaresan, S.; van den Akker, H. Simulation of mass-loading effects in gas-solid cyclone separators. *Powder Technol.* **2006**, *163*, 59–68. [[CrossRef](#)]

117. Ho, C.; Sommerfeld, M. Modelling of micro-particle agglomeration in turbulent flows. *Chem. Eng. Sci.* **2002**, *57*, 3073–3084. [[CrossRef](#)]
118. Ho, C.; Sommerfeld, M. Numerische Berechnung der Staubabscheidung im Gaszyklon unter Berücksichtigung der Partikelagglomeration. *Chem. Ing. Tech.* **2005**, *77*, 282–290. [[CrossRef](#)]
119. Breuer, M.; Almohammed, N. Modeling and simulation of particle agglomeration in turbulent flows using a hard-sphere model with deterministic collision detection and enhanced structure models. *Int. J. Multiph. Flow* **2015**, *73*, 171–206. [[CrossRef](#)]
120. Almohammed, N.; Breuer, M. Modeling and simulation of agglomeration in turbulent particle-laden flows: A comparison between energy-based and momentum-based agglomeration models. *Powder Technol.* **2016**, *294*, 373–402. [[CrossRef](#)]
121. Sommerfeld, M. Validation of a stochastic Lagrangian modelling approach for inter-particle collisions in homogeneous isotropic turbulence. *Int. J. Multiph. Flow* **2001**, *27*, 1829–1858. [[CrossRef](#)]
122. Gronald, G.; Staudinger, G. Investigations on agglomeration in gas cyclones. In Proceedings of the World Congress on Particle Technology, Tsukuba, Japan, 23–27 April 2006.
123. Meier, H.; Mori, M. Gas-solid flow in cyclones: The Eulerian-Eulerian approach. *Comput. Chem. Eng.* **1998**, *22*.
124. Vegini, A.; Meier, H.; Iess, J.; Mori, M. Computational Fluid Dynamics (CFD) Analysis of Cyclone Separators Connected in Series. *Ind. Eng. Chem. Res.* **2008**, *47*, 192–200. [[CrossRef](#)]
125. Meier, H.; Vegini, A.; Mori, M. Four-Phase Eulerian-Eulerian Model for Prediction of Multiphase Flow in Cyclones. *J. Comput. Multiph. Flows* **2011**, *3*, 93–105. [[CrossRef](#)]
126. Costa, K.; Sgrott, O.; Decker, R.; Reinehr, E.; Martignoni, W.; Meier, H. Effects of phases' numbers and solid-solid interactions on the numerical simulations of cyclones. *Chem. Eng. Trans.* **2013**, *32*, 1567–1572. [[CrossRef](#)]
127. Sgrott, O.; Noriler, D.; Wiggers, V.; Meier, H. Cyclone optimization by COMPLEX method and CFD simulation. *Powder Technol.* **2015**, *277*, 11–21. [[CrossRef](#)]
128. Sgrott, O.; Costa, K.; Noriler, D.; Wiggers, V.; Martignoni, W.; Meier, H. Cyclones' project optimization by combination of an inequality constrained problem and computational fluid dynamics techniques (CFD). *Chem. Eng. Trans.* **2013**, *32*, 2011–2016. [[CrossRef](#)]
129. Luciano, R.; Silva, B.; Rosa, L.; Meier, H. Multi-objective optimization of cyclone separators in series based on computational fluid dynamics. *Powder Technol.* **2018**, *325*, 452–466. [[CrossRef](#)]
130. Qian, F.; Huang, Z.; Chen, G.; Zhang, M. Numerical study of the separation characteristics in a cyclone of different inlet particle concentrations. *Comput. Chem. Eng.* **2007**, *31*, 1111–1122. [[CrossRef](#)]
131. Kharoua, N.; Khezzer, L.; Nemouchi, Z. Study of the Pressure Drop and Flow Field in Standard Gas Cyclone Models Using the Granular Model. *Int. J. Chem. Eng.* **2011**, *2011*, 1–11. [[CrossRef](#)]
132. Shi, L.; Bayless, D.; Kremer, G.; Stuart, B. CFD simulation of the influence of temperature and pressure on the flow pattern in cyclones. *Ind. Eng. Chem. Res.* **2006**, *45*, 7667–7672. [[CrossRef](#)]
133. Gimbut, J.; Chuah, T.; Fakhru'l-Razi, A.; Choong, T.S. The influence of temperature and inlet velocity on cyclone pressure drop: A CFD study. *Chem. Eng. Process. Process Intensif.* **2005**, *44*, 7–12. [[CrossRef](#)]
134. Shin, M.; Kim, H.; Jang, D.; Chung, J.; Bohnet, M. A numerical and experimental study on a high efficiency cyclone dust separator for high temperature and pressurized environments. *Appl. Therm. Eng.* **2005**, *25*, 1821–1835. [[CrossRef](#)]
135. Duan, L.; Wu, X.; Zhongli, J. The influence of temperature on the entropy generation of cyclone separator. In Proceedings of the 11th International Conference on Fluidized Bed Technology, Beijing, China, 1 May 2014; pp. 923–928.
136. Siadaty, M.; Kheradmand, S.; Ghadiri, F. Study of inlet temperature effect on single and double inlets cyclone performance. *Adv. Powder Technol.* **2017**, *28*, 1459–1473. [[CrossRef](#)]
137. Duan, L.; Wu, X.; Ji, Z.; Fang, Q. Entropy generation analysis on cyclone separators with different exit pipe diameters and inlet dimensions. *Chem. Eng. Sci.* **2015**, *138*, 622–633. [[CrossRef](#)]
138. Duan, L.; Wu, X.; Ji, Z.; Xiong, Z.; Zhuang, J. The flow pattern and entropy generation in an axial inlet cyclone with reflux cone and gaps in the vortex finder. *Powder Technol.* **2016**, *303*, 192–202. [[CrossRef](#)]
139. Gimbut, J.; Chuah, T.; Choong, T.; Fakhru'l-Razi, A. A CFD Study on the Prediction of Cyclone Collection Efficiency. *Int. J. Comput. Methods Eng. Sci. Mech.* **2005**, *6*, 161–168. [[CrossRef](#)]

140. Mothilal, T.; Pitchandi, K. Influence of inlet velocity of air and solid particle feed rate on holdup mass and heat transfer characteristics in cyclone heat exchanger. *J. Mech. Sci. Technol.* **2015**, *29*, 4509–4518. [[CrossRef](#)]
141. Mothilal, T.; Pitchandi, K. Computational fluid dynamic analysis on the effect of particles density and body diameter in a tangential inlet cyclone heat exchanger. *Therm. Sci.* **2017**, *21*, 2883–2895. [[CrossRef](#)]
142. Cristea, E.; Conti, P. Coupled 3-D CFD-DDPM numerical simulation of turbulent swirling gas-particle flow within cyclone suspension preheater of cement kilns. Proceedings of the ASME 2016 Fluids Engineering Division Summer Meeting collocated with the ASME 2016 Heat Transfer Summer Conference and the ASME 2016 14th International Conference on Nanochannels, Microchannels, and Minichannels, Washington, DC, USA, 10–2013;14 July 2016. [[CrossRef](#)]
143. Cristea, E.; Conti, P. Hybrid Eulerian Multiphase-Dense Discrete Phase Model Approach for Numerical Simulation of Dense Particle-Laden Turbulent Flows Within Vertical Multi-Stage Cyclone Heat Exchanger. In Proceedings of the ASME 2018 5th Joint US-European Fluids Engineering Division Summer Meeting, Montreal, QC, Canada, 15–20 July 2018. [[CrossRef](#)]
144. Mikulčić, H.; Vujanović, M.; Ashhab, M.; Duić, N. Large eddy simulation of a two-phase reacting swirl flow inside a cement cyclone. *Energy* **2014**, *75*, 89–96. [[CrossRef](#)]
145. Wasilewski, M. Analysis of the effects of temperature and the share of solid and gas phases on the process of separation in a cyclone suspension preheater. *Sep. Purif. Technol.* **2016**, *168*, 114–123. [[CrossRef](#)]
146. Schiller, L.; Naumann, A. Über die grundlegenden berechnungen bei der schwerkraftaufbereitung. *Vereines Dtsch. Ingenieure* **1933**, *77*, 318–320.
147. Masnadi, M.; Grace, J.; Elyasi, S.; Bi, X. Distribution of multi-phase gas-solid flow across identical parallel cyclones: Modeling and experimental study. *Sep. Purif. Technol.* **2010**, *72*, 48–55. [[CrossRef](#)]
148. Grace, J. Maldistribution of flow through parallel cyclones in circulating fluidized beds. In Proceedings of the 9th International Conference on Circulating Fluidized Beds, CFB 2008, in Conjunction with the 4th International VGB Workshop on Operating Experience with Fluidized Bed Firing Systems, Hamburg, Germany, 13–16 May 2008; Code 106582.
149. Kim, T.; Choi, J.; Shun, D.; Kim, S.; Kim, S.; Grace, J. Wear of water walls in a commercial circulating fluidized bed combustor with two gas exits. *Powder Technol.* **2007**, *178*, 143–150. [[CrossRef](#)]
150. Zhou, X.; Cheng, L.; Wang, Q.; Luo, Z.; Cen, K. Non-uniform distribution of gas-solid flow through six parallel cyclones in a CFB system: An experimental study. *Particuology* **2012**, *10*, 170–175. [[CrossRef](#)]
151. Zhang, N.; Lu, B.; Wang, W.; Li, J. 3D CFD simulation of hydrodynamics of a 150MWe circulating fluidized bed boiler. *Chem. Eng. J.* **2010**, *162*, 821–828. [[CrossRef](#)]
152. Jiang, Y.; Qiu, G.; Wang, H. Modelling and experimental investigation of the full-loop gas-solid flow in a circulating fluidized bed with six cyclone separators. *Chem. Eng. Sci.* **2014**, *109*, 85–97. [[CrossRef](#)]
153. Wang, W.; Li, J. Simulation of gas-solid two-phase flow by a multi-scale CFD approach of the EMMS model to the sub-grid level. *Chem. Eng. Sci.* **2007**, *62*, 208–231. [[CrossRef](#)]



© 2019 by the authors. Licensee MDPI, Basel, Switzerland. This article is an open access article distributed under the terms and conditions of the Creative Commons Attribution (CC BY) license (<http://creativecommons.org/licenses/by/4.0/>).